J. Fluid Mech. (2003), *vol.* 497, *pp.* 253–287.
DOI: 10.1017/S0022112003006657 Printed in the United Kingdom

Effects of surface waves on a turbulent current over a smooth or rough seabed

By ZHENHUA HUANG AND CHIANG C. MEI

Department of Civil and Environmental Engineering, Massachusetts Institute of Technology, Cambridge MA, 02139, USA

(Received 19 January 2003 and in revised form 17 August 2003)

Laboratory experiments by earlier authors have shown that the near-surface velocity of an otherwise uniform current is reduced by following waves, but is increased by opposing waves. By a boundary-layer analysis with depth-dependent eddy viscosities, we show analytically that this is the consequence of second-order effects of wave–current interaction. Physical effects of waves on the current profile due to the moving free surface, wave attenuation and convective inertia are discussed. Comparisons with available experiments for smooth and rough seabeds are discussed. New predictions of the longitudinal variations along the current are made.

1. Introduction

Fine sediments on the bottom of a shallow lake or sea can be resuspended by waves and transported by the current. Since these particles can be carriers of contaminants and nutrients, their distribution is crucial to the health of the water body. Quantitative understanding of the mutual influence between waves, current and wind is therefore of basic importance to the prediction of biological and/or chemical processes in shallow water. Omitting the direct effects of wind, Grant & Madsen (1979, 1986) have studied the effects of turbulence by a simple eddy-viscosity model, with attention focused on the region close to the seabed where sediment transport is often the most important. Based on experiments by Bakker & Doorn (1978) and Mathisen & Madsen (1996*a*, *b*) and by others, they find that a current followed by waves experiences a reduction of speed near the bed, hence an increase of the apparent roughness. The record of Bakker & Doorn (1978) also shows a notable reduction of current velocity near the water surface. Later Kemp & Simons (1982, 1983), and Klopman (1994, 1997) reported full-depth profiles by similar experiments and showed that the near-surface velocity of a current is increased (reduced) if opposed (followed) by waves; consistent reduction near the bed was observed for wave-oppposing currents. In experiments by Nepf *et al.* (1995) on Langmuir circulation in a channel of finite width, mechanically generated breaking waves along a steady current also retard the current near the free surface along the centreplane of the flume.

Since very fine sediments in lakes or shallow seas can be readily resuspended far above the bottom, the mean velocity distribution in the entire depth is of importance to their transport. Theoretical models for the prediction of wave–current interaction should therefore also include the region near the free surface. An eddy-viscosity model for this problem has been attempted by Nielsen & You (1996). Several *ad hoc* assumptions were added and the agreement with measured data is not

very satisfactory. Dingemans *et al.* (1996) attributed the wave-induced change of the Eulerian mean velocity to Langmuir circulation induced by the lateral boundaries of the wave tank. The results of their three-dimensional computations based on a $k-\varepsilon$ model agree reasonably well with the measurement of Klopman only for waves following, but not opposing, the current. Allowing the current to be as strong as the phase velocity of waves, Groeneweg & Klopman (1998) treated the two-dimensional problem by combining the method of generalized Lagrangian mean (GLM) and a numerical turbulence model. By an empirical estimate of the eddy viscosity and numerical computations, they found good agreement between the computed and measured profiles of the longitudinal velocity for both coflowing and counterflowing currents of Klopman (1994). Their method was further extended by Groeneweg & Battjes (2003) to study the sidewall effects in the three-dimensional motion in a long flume of finite width. Transverse circulation due to the presence of the vertical sidewalls was calculated, but was found to have only weak effects on the longitudinal velocity profiles.

Since simple eddy-viscosity models facilitate analytical examination of the physical phenomenon, they have been used in early studies of wave generation by wind. Townsend (1972) proposed an eddy-viscosity model in which the mixing length is measured from the moving water surface. Thus the eddy viscosity near the sea surface is modified by waves and depends on time. In consequence, the mean wind velocity near the water surface is significantly affected. Similar ideas about the wave-modified mixing length have been used by Jacobs (1987) and Van Duin & Janssen (1992). Essentially equivalently Miles (1993) assumed that the eddy viscosity is conserved along the streamlines. The common feature of these models is that the mixing length in the air flow is measured from the moving air–water interface, which restricts the size of local turbulent eddies. As a result the eddy viscosity is now the sum of a steady part and a transient part; the latter is associated with free-surface oscillations. While these models are still crude and heuristic representations of the complex physics of turbulence, they can help mimic the averaged motion without elaborate numerical computations.

Based on existing laboratory data on waves in finite depth, smooth and rough beds must be distinguished. Over a smooth bed, a steady current of the assumed magnitude is usually turbulent as the Reynolds threshold $\langle \bar{u}_c^* \rangle h/\nu > 2100$ is easily superseded (for example, by a typical case with $\langle \bar{u}_c^* \rangle > 21\,\mathrm{cm\,s^{-1}}$, and $h = 10\,\mathrm{cm}$). However, a pure wave with comparable orbital velocity becomes turbulent in the bed boundary layer only if $Re_w \equiv \omega a_b^2/\nu > N \times 10^4$ where ω is the wave frequency and a_b the orbital amplitude just above the smooth bed. The coefficient N varies from 1.26 (Jonsson 1966) to about 30 (Kamphuis 1975). Laboratory waves often fall below this threshold (e.g., $a_b = 5\,\mathrm{cm}$ and $\omega = 2\pi\,\mathrm{s^{-1}}$ gives $Re_w = 1.57 \times 10^4$). In this case, turbulence in the bed wave boundary layer is dominated by the pre-existing current. For a rough bed, it is known that the ratio a_b/k_N, where k_N is the Nikuradse sand grain size, is another important factor. When a_b/k_N decreases, the threshold Re_w decreases. Only above a certain transitional range of Re_w is the bottom flow fully turbulent (see, Kamphuis 1975 or Sleath 1984). By defining $\delta = O(\kappa u_f/\omega)$ as the thickness of the wave boundary layer (Kajiura 1968), and $u_f = \omega a_b \sqrt{f_w/2}$, it follows that $\delta/k_N = O[(\kappa\sqrt{f_w/2})(a_b/k_N)]$. Only when $\delta/k_N (\propto a_b/k_N) \gg 1$, are the roughness elements deeply buried inside the fully turbulent zone which can be described as the boundary layer. For such cases which are relevant to most field-scale applications, a theoretical model for the wave–current boundary layer has been developed by Grant & Madsen (1979, 1986) by introducing an enhanced eddy

viscosity. Their scheme has been found useful for quantitative modelling of coastal dynamics (Tang & Grimshaw 1999).

We shall give a boundary-layer theory incorporating eddy-viscosity models which account for the moving free surface and different seabed conditions. In particular, the eddy viscosity ν_e diminishes to zero at both the moving free surface and the seabed and is the largest at mid-core. For a smooth seabed, ν_e diminishes continuously from the core. For a rough bed, a different eddy viscosity linear in height with a larger friction velocity is assumed in the bed wave boundary layer (BWBL), and is discontinuous at the upper edge of the layer. After normalization and order estimates, the governing equation for the wave-perturbed current velocity in the core is derived by including the effects of wave-induced Reynolds stress, and energy dissipation. While the first-order oscillatory motion gives the dissipation rate in BWBL, the second-order mean motion gives rise to wave Reynolds stress affecting the core current. For both a smooth bed and a rough bed where the roughness elements are deeply immersed inside the wave boundary layer, a second-order analysis also provides the lower boundary value for the core current. Near the free surface, we first show that the wave boundary layer is unimportant. A second-order analysis gives the mean shear stress at the mean sea-level. With this as the upper boundary condition the core current is solved analytically. Determination of the friction velocities will be discussed. Quantitative predictions of the current profiles affected by waves in the same or opposite direction will be compared with experimental data at one station. For a smooth bed the agreement is excellent. For a rough bed, existing laboratory data are all for roughness either of moderate a_b/k_N, or formed by well separated strips. For these beds, the boundary-layer model is tenuous at best. Nevertheless we shall show that good agreement is still found for the damping rate and the velocity profiles can also be predicted well if empirical fitting at the lower boundary is made. Physical mechanisms responsible for current reduction or increase near the surface will be explained. For future experiments, we also present predictions of the spatial variation of current profiles in the direction of flow.

2. Formulation

We shall use asterisks to distinguish dimensional from dimensionless variables, and from other parameters. Let waves propagate in the positive x^*-direction, and the mean current either follows or opposes waves in the positive or negative x^*-direction, respectively.

Let $\{u_i^*\} \equiv \{u^*, w^*\}$ be the velocity components in $x_i^* = \{x^*, z^*\}$ directions, and p^* the dynamic pressure, where the total pressure is $p^* - \rho g z^*$. The two-dimensional motion is governed by the Reynolds equations

$$\frac{\partial u_j^*}{\partial x_j^*} = 0, \tag{2.1}$$

$$\rho \frac{\partial u_i^*}{\partial t^*} + \rho \frac{\partial u_i^* u_j^*}{\partial x_j^*} = -\frac{\partial p^*}{\partial x_i^*} + \frac{\partial \tau_{ij}^*}{\partial x_j^*}, \tag{2.2}$$

where ρ is the water density. The Reynolds stress is modelled by

$$\tau_{ij}^* = \rho \nu_e \left(\frac{\partial u_i^*}{\partial x_j^*} + \frac{\partial u_j^*}{\partial x_i^*} \right). \tag{2.3}$$

On the free surface $z^* = \eta^*(x^*, t^*)$, the kinematic condition requires

$$\frac{\partial \eta^*}{\partial t^*} + u^* \frac{\partial \eta^*}{\partial x^*} - w^* = 0, \quad z^* = \eta^*. \tag{2.4}$$

Assuming no wind, the shear and normal stresses must vanish on the moving free surface,

$$-[-(p^* - \rho g \eta^*) + \tau_{xx}^*] \frac{\partial \eta^*}{\partial x^*} + \tau_{xz}^* = 0, \qquad z^* = \eta^*; \tag{2.5}$$

$$[-(p^* - \rho g \eta^*) + \tau_{zz}^*] - \tau_{xz}^* \frac{\partial \eta^*}{\partial x^*} = 0, \quad z^* = \eta^*. \tag{2.6}$$

We define the seabed $z^* = -h + z_B$, to be the depth where no slippage occurs,

$$u^* = w^* = 0, \quad z^* = -h + z_B, \tag{2.7}$$

where z_B is the hydraulic roughness whose determination will be discussed later.

Borrowing the ideas of Townsend (1972) and Jacobs (1987) in their studies of wind near the wavy sea surface, we adopt the following eddy-viscosity model for the core region outside the BWBL

$$\nu_e \equiv \nu_c = -\kappa u_{fc}(z^* - \eta^*)\left(1 + \frac{z^*}{h}\right), \qquad -h + \delta < z^* < \eta^*, \tag{2.8}$$

where η^* is the water surface displacement, $\kappa = 0.4$ is the von Kármán constant, h the water depth, u_{fc} the friction velocity and δ is the thickness of BWBL to be determined.

Near the seabed, we distinguish three cases.

Case A. Laminar wave boundary layer over a smooth bed. $Re_w < N \times 10^4$ and $a_b/k_N \to \infty$. Turbulence is dominated by the current, and the eddy viscosity is the near-bottom approximation of (2.8),

$$\nu_e \equiv \nu_b = \kappa u_{fc}(h + z^*), \qquad -h + z_B < z^* = -h + \delta, \quad \text{smooth bed.} \tag{2.9}$$

Thus the eddy viscosity is continuous everywhere.

Case B. Rough seabed with $(\delta/k_N, a_b/k_N) \gg 1$. Wave-induced turbulence can be described by a boundary-layer theory. A larger eddy viscosity accounting for contributions by both waves and currents is assumed,

$$\nu_e \equiv \nu_b = \kappa u_{fb}(h + z^*), \qquad -h + z_B < z^* = -h + \delta, \quad \text{rough bed,} \tag{2.10}$$

where $u_{fb} \neq u_{fc}$ is the friction velocity combining the effects of both current and waves. This friction velocity u_{fb} will be determined by the procedure of Grant & Madsen. Clearly, ν_e is discontinuous at the edge of BWBL.

Case C. Rough seabed with moderate (δ/k_N or a_b/k_N). Wave-induced turbulence is two- or three-dimensional and cannot be described accurately by boundary-layer approximation. The threshold for a_b/k_N is around 10 to 115, according to Kamphuis (1975), Sleath (1984), Mathisen & Madsen (1996*a*, *b*). Beds roughened by well-separated strips fall into this class.

We shall only consider waves of gentle slope so that

$$\epsilon \equiv ka = \ll 1 \tag{2.11}$$

where a and k are the characteristic wave amplitude and wavenumber, respectively. In addition, the basic current is assumed to be comparable to the wave orbital velocity,

$$\bar{u}^* \sim \tilde{u}^* = O(\epsilon C), \quad C = \omega/k = \text{phase velocity.} \tag{2.12}$$

where $\bar{u}^*$ and $\tilde{u}^*$ are the mean and fluctuating velocity of the water motion, respectively.

An *a priori* order estimate can be made of the friction velocities u_{fc} of the core current and u_{fb} of the bed boundary layer. For u_{fc}, the knowledge of open channel flows $\bar{u}_0^*$ given by

$$\bar{u}_0^* = \pm \frac{u_{fc}}{\kappa} \ln \left(\frac{z^* + h}{z_B} \right) \tag{2.13}$$

is relevant. The plus sign is for the positive current (from left to right) and the minus sign for the negative current (from right to left). The friction velocity u_{fc} is related to the friction factor f_c, commonly defined by

$$\rho (u_{fc})^2 = \rho \frac{f_c}{2} \langle \bar{u}_0^* \rangle^2, \tag{2.14}$$

where $\langle \bar{u}_0^* \rangle$ stands for the depth average of the basic current. It follows that

$$u_{fc} = \sqrt{\frac{f_c}{2}} \, |\langle \bar{u}_0^* \rangle| \,, \tag{2.15}$$

The common empirical value of the friction factor is about $f_c \sim 0.01$. In view of the assumption that $O(\langle \bar{u}^* \rangle) = O(\tilde{u}^*) = O(\epsilon C)$, we shall regard $u_{fc}/\tilde{u}^* = O(\epsilon)$, or equivalently,

$$u_{fc} = O(\epsilon^2 C). \tag{2.16}$$

Equation (2.13) is consistent with (2.16) if

$$\ln \frac{h}{z_B} = O\left(\frac{1}{\epsilon} \right), \tag{2.17}$$

which we shall assume. Note that the corresponding shear rate of the basic current is

$$\frac{h}{C} \frac{\partial \bar{u}_0^*}{\partial z^*} = \pm \frac{u_{fc}}{\kappa C} \frac{h}{z^* + h}, \tag{2.18}$$

which is $O(\epsilon^2)$ when $z^* + h = O(h)$, but of order $O(1)$ when $(z^* + h)/h = O(\epsilon^2)$, i.e. near or inside the bed boundary layer. This difference is associated with the logarithmic variations near the bottom.

Though different in numerical values, the friction velocity in the BWBL must be of the same order of magnitude as those in the core current. This is because waves and current are of comparable strength here. Hence, we estimate

$$\frac{u_{fb}}{C} \sim \frac{u_{fc}}{C} = O(\epsilon^2), \tag{2.19}$$

which can be checked after applying the procedure of Grant & Madsen (1979, 1986).

3. Normalization by core scales

We shall first normalize all equations by the scales appropriate for the core. In the BWBL, modification will later be made so that the vertical coordinate will be renormalized by the boundary-layer thickness.

Let us denote the characteristic wavenumber by $k = 2\pi/\text{wavelength}$, the angular frequency by $\omega = 2\pi/T$, and the phase speed by $C = \omega/k$ according to the linearized theory. The normalized outer variables (without asterisks) are defined as follows:

$$t = \omega t^*, \quad (x, z, \eta) = k(x^*, z^*, \eta^*), \quad u_i = u_i^*/C, \quad (\tau_{ij}, p) = (\tau_{ij}^*, p^*)/\rho C^2. \tag{3.1}$$

Conservation of mass requires

$$\frac{\partial u}{\partial x}+\frac{\partial w}{\partial z}=0. \tag{3.2}$$

In the momentum conservation laws, convective inertia terms are written in two equivalent forms,

$$\frac{\partial u}{\partial t}+\frac{\partial (uu)}{\partial x}+\frac{\partial (uw)}{\partial z}\equiv \frac{\partial u}{\partial t}+\frac{\partial E}{\partial x}+w\Omega =-\frac{\partial p}{\partial x}+\frac{\partial \tau_{xx}}{\partial x}+\frac{\partial \tau_{xz}}{\partial z}, \tag{3.3}$$

$$\frac{\partial w}{\partial t}+\frac{\partial (uw)}{\partial x}+\frac{\partial (ww)}{\partial z}\equiv \frac{\partial w}{\partial t}+\frac{\partial E}{\partial z}-u\Omega =-\frac{\partial p}{\partial z}+\frac{\partial \tau_{xz}}{\partial x}+\frac{\partial \tau_{zz}}{\partial z}, \tag{3.4}$$

where

$$E=\tfrac{1}{2}(u^2+w^2) \tag{3.5}$$

is the kinetic energy, and

$$\Omega =\frac{\partial u}{\partial z}-\frac{\partial w}{\partial x} \tag{3.6}$$

is the vorticity component in the y-direction. The dynamic pressure p is related to the total pressure P by $p=P+(gk/\omega^2)z$. Using the eddy viscosity modelled by (2.8) in the core and (2.10) in the bed boundary layer, the dimensionless Reynolds stresses are related to the strain rates by,

$$\tau_{xx}=2\alpha\epsilon^2 S\frac{\partial u}{\partial x},\quad \tau_{zz}=2\alpha\epsilon^2 S\frac{\partial w}{\partial z},\quad \tau_{xz}=\alpha\epsilon^2 S\left(\frac{\partial u}{\partial z}+\frac{\partial w}{\partial x}\right), \tag{3.7}$$

where S is the shape factor of the eddy viscosity,

$$S=\begin{cases} S_c=-(z-\eta)\left(1+\dfrac{z}{kh}\right), & \text{core},\\ S_b=1+\dfrac{z}{kh}, & \text{BWBL}, \end{cases} \tag{3.8}$$

and α is the dimensionless friction velocity,

$$\alpha=\alpha_c=\kappa u_{fc}/C\epsilon^2,\quad \text{core}, \tag{3.9}$$

$$\alpha=\alpha_b=\begin{cases}\kappa u_{fc}/C\epsilon^2, & \text{BWBL, Case A},\\ \kappa u_{fb}/C\epsilon^2, & \text{BWBL, Cases B}.\end{cases} \tag{3.10}$$

In accordance with (2.19), we have $O(\alpha_c)=O(\alpha_b)=O(1)$, We further rewrite S_c in (3.8) as

$$S_c=\bar{S}_c+\hat{S}_c\eta, \tag{3.11}$$

so that $\bar{S}_c$ is the time mean of S_c and $\hat{S}_c\eta$ is the surface distortion of the eddy viscosity, where

$$\bar{S}_c=-z\left(1+\frac{z}{kh}\right),\quad \hat{S}_c=1+\frac{z}{kh}. \tag{3.12}$$

Note from (3.7) that the Reynolds stresses are of order $O(\epsilon^3)$ in the core region.

For later use, we give the vorticity equation by eliminating the pressure p from the momentum equations (3.3) and (3.4)

$$\frac{\partial \Omega}{\partial t}+u\frac{\partial \Omega}{\partial x}+w\frac{\partial \Omega}{\partial z}=\Pi \tag{3.13}$$

where

$$\Pi \equiv \frac{\partial}{\partial z}\left(\frac{\partial \tau_{xx}}{\partial x}+\frac{\partial \tau_{xz}}{\partial z}\right)-\frac{\partial}{\partial x}\left(\frac{\partial \tau_{xz}}{\partial x}+\frac{\partial \tau_{zz}}{\partial z}\right). \tag{3.14}$$

We now introduce averages with respect to a wave period, and refer to all period averages† as mean quantities from here on. Let us separate the mean current and the wave motion so that

$$\begin{gathered}(u, w, p, \eta, \Omega)=(\bar{u}, \bar{w}, \bar{p}, \bar{\eta}, \bar{\Omega})+(\tilde{u}, \tilde{w}, \tilde{p}, \tilde{\eta}, \tilde{\Omega}),\\ (\tau_{xx}, \tau_{xz}, \tau_{zz})=(\bar{\tau}_{xx}, \bar{\tau}_{xz}, \bar{\tau}_{zz})+(\tilde{\tau}_{xx}, \tilde{\tau}_{xz}, \tilde{\tau}_{zz}),\end{gathered} \tag{3.15}$$

where quantities with bars represent the time mean and those with tildes the wave motion. By taking the time-average of the governing equations (3.2),(3.3) and (3.4), we obtain the governing equations of the current

$$\frac{\partial \bar{u}}{\partial x}+\frac{\partial \bar{w}}{\partial z}=0, \tag{3.16}$$

$$\frac{\partial(\bar{u}\bar{u})}{\partial x}+\frac{\partial(\bar{u}\bar{w})}{\partial z}+\frac{\partial \bar{E}_w}{\partial x}+\overline{\tilde{w}\tilde{\Omega}}=-\frac{\partial \bar{p}}{\partial x}+\frac{\partial \bar{\tau}_{xx}}{\partial x}+\frac{\partial \bar{\tau}_{xz}}{\partial z}, \tag{3.17}$$

$$\frac{\partial(\bar{u}\bar{w})}{\partial x}+\frac{\partial(\bar{w}\bar{w})}{\partial z}+\frac{\partial \bar{E}_w}{\partial z}-\overline{\tilde{u}\tilde{\Omega}}=-\frac{\partial \bar{p}}{\partial z}+\frac{\partial \bar{\tau}_{xz}}{\partial x}+\frac{\partial \bar{\tau}_{zz}}{\partial z}, \tag{3.18}$$

where $\bar{E}_w$ is the wave kinetic energy

$$\bar{E}_w=\tfrac{1}{2}(\overline{\tilde{u}^2}+\overline{\tilde{w}^2})=O(\epsilon^2) \tag{3.19}$$

The wave-averaged Reynolds stresses are obtained by taking the time-average of (3.7), which are, in the core,

$$\bar{\tau}_{xx}=2\alpha_c\epsilon^2\bar{S}_c\frac{\partial \bar{u}}{\partial x}+2\alpha_c\epsilon^2\hat{S}_c\overline{\tilde{\eta}\frac{\partial \tilde{u}}{\partial x}}, \tag{3.20}$$

$$\bar{\tau}_{zz}=2\alpha_c\epsilon^2\bar{S}_c\frac{\partial \bar{w}}{\partial z}+2\alpha_c\epsilon^2\hat{S}_c\overline{\tilde{\eta}\frac{\partial \tilde{w}}{\partial z}}, \tag{3.21}$$

$$\bar{\tau}_{xz}=\alpha_c\epsilon^2\bar{S}_c\left(\frac{\partial \bar{u}}{\partial z}+\frac{\partial \bar{w}}{\partial x}\right)+\alpha_c\epsilon^2\hat{S}_c\overline{\tilde{\eta}\left(\frac{\partial \tilde{u}}{\partial z}+\frac{\partial \tilde{w}}{\partial x}\right)}. \tag{3.22}$$

In the boundary layer, the wave-averaged Reynolds stresses are obtained simply by replacing α_c with α_b, $\bar{S}_c$ with S_b and setting $\hat{S}_c$ to zero.

4. Basic current

In addition to the well-known result (2.13) we summarize the salient relations of the basic current for later convenience. Let subscript $()_0$ signify the basic current

$$\bar{u}=\epsilon\bar{u}_0, \quad \bar{w}_0=0, \quad \bar{p}=\epsilon\bar{p}_0. \tag{4.1}$$

Omitting the wave-perturbed parts in (3.17), we obtain the equation governing $\bar{u}_0$

$$\frac{\partial \bar{p}_0}{\partial x}=\epsilon^2\alpha_0\frac{\partial}{\partial z}\left(\bar{S}_c\frac{\partial \bar{u}_0}{\partial z}\right) \quad \text{where} \quad \alpha_0=\kappa u_{fc}/C\epsilon^2, \tag{4.2}$$

† These are period averages of stochastic averages.

to which the solution is (2.13). In (4.2), $\bar{p}_0$ is constant in depth from the vertical momentum equation. The pressure gradient of the basic current can be identified with the normalized friction velocity by

$$-\frac{\partial \bar{p}_0}{\partial x} = \pm\epsilon^3 \frac{\alpha_0^2}{\kappa^2}. \tag{4.3}$$

For later use, we note that the mean shear stress of the basic current has the following form

$$(\bar{\tau}_{xz})_0 = \pm\epsilon^4 \frac{\alpha_0^2}{\kappa^2}\left(\frac{-z}{kh}\right) \tag{4.4}$$

and is $O(\epsilon^4)$.

5. Length scale of wave attenuation

Owing to disspation, waves will attenuate in x. Since other mean quantities may in turn be affected, we must first ascertain the scale of attenuation by considering the mechancial energy in waves.

Let the leading-order surface displacement of the surface wave be

$$\widetilde{\eta} = \epsilon\left(\frac{A}{2}e^{i\theta} + \text{c.c.}\right) + O(\epsilon^2), \tag{5.1}$$

where $\epsilon A = O(\epsilon)$ is the dimensionless wave amplitude and $\theta = x - t$ the wave phase. Since, by assumption, the eddy viscosity is of $O(\epsilon^2)$ and the rotational core current of $O(\epsilon)$, the leading-order wave field is irrotational,

$$\widetilde{u} = \epsilon\left(\frac{A}{2}\frac{\cosh(kh+z)}{\sinh(kh)}e^{i\theta} + \text{c.c.}\right) + O(\epsilon^2), \tag{5.2}$$

$$\widetilde{w} = \epsilon\left(-i\frac{A}{2}\frac{\sinh(kh+z)}{\sinh(kh)}e^{i\theta} + \text{c.c.}\right) + O(\epsilon^2), \tag{5.3}$$

$$\widetilde{p} = \epsilon\left(\frac{A}{2}\frac{\cosh(kh+z)}{\sinh(kh)}e^{i\theta} + \text{c.c.}\right) + O(\epsilon^2). \tag{5.4}$$

Using standard arguments we can derive from the conservation laws the equation of mechanical energy in waves

$$\frac{\epsilon^2}{2}\int_{-kh+kz_B}^{-kh+k\delta} \alpha_b S_b \overline{\left(\frac{\partial \widetilde{u}_i}{\partial x_j} + \frac{\partial \widetilde{u}_j}{\partial x_i}\right)^2}\,dz + \frac{\epsilon^2}{2}\int_{-kh+k\delta}^{0} \alpha_c \bar{S}_c \overline{\left(\frac{\partial \widetilde{u}_i}{\partial x_j} + \frac{\partial \widetilde{u}_j}{\partial x_i}\right)^2}\,dz = -\frac{\partial}{\partial x}\int_{-kh+kz_B}^{0} \overline{\widetilde{u}\widetilde{p}}\,dz, \tag{5.5}$$

where $k\delta = O(\epsilon^2)$ is the dimensionless thickness of the BWBL. For reference, a derivation is sketched in Appendix A. Note that there are two depth integrals corresponding to the BWBL and the core. In the core $\bar{S}_c = O(1)$, we can ignore the BWBL and obtain

$$\overline{\widetilde{u}\widetilde{p}} \propto \epsilon^2 AA^*, \quad \int_{-kh}^{0} \bar{S}_c \overline{\left(\frac{\partial \widetilde{u}_i}{\partial x_j} + \frac{\partial \widetilde{u}_j}{\partial x_i}\right)^2}\,dz \propto \epsilon^2 AA^*, \tag{5.6}$$

where A^* is the complex conjugate of A. Because $S_b = O(k\delta)$, balance of the transient acceleration and the oscillatory viscous stress implies that $k\delta = O(\epsilon^2)$. Thus the

integral across the bed boundary layer is

$$\int_{-kh+kz_B}^{k\delta} S_b \overline{\left(\frac{\partial \tilde{u}_i}{\partial x_j}+\frac{\partial \tilde{u}_j}{\partial x_i}\right)^2}\,\mathrm{d}z \propto \epsilon^2 AA^*. \tag{5.7}$$

Two inferences may be made. First, dissipation in the two regions are comparably important; weak shear in the core is compensated by the large eddy viscosity there. Secondly, the length scale of horizontal length scale of attenuation is $O(\epsilon^{-2})$ times that of the wavelength. This should affect all mean quantities associated with wave disturbances. Therefore, we introduce the slow coordinate $x_2 = \epsilon^2 x$. The x derivative of every wave-periodic mean $\bar{f}$ is

$$\frac{\partial \bar{f}}{\partial x} = \epsilon^2 \frac{\partial \bar{f}}{\partial x_2} = O(\epsilon^2 \bar{f}). \tag{5.8}$$

Also, (5.5) should yield formally

$$\frac{\partial AA^*}{\partial x_2} = -\beta AA^*, \tag{5.9}$$

where $\beta > 0$ is the wave energy dissipation rate, which will be calculated explicitly later.

6. Core

6.1. *Order estimate of wave-induced core current*

Extending (4.1), we express the total mean motion as the sum of the basic and wave-induced parts

$$\bar{u} = \epsilon \bar{u}_0 + \mu_1(\epsilon)\bar{u}_c', \quad \bar{w} = \mu_2(\epsilon)\bar{w}_c', \quad \bar{p} = \epsilon \bar{p}_0 + \mu_1(\epsilon)\bar{p}_c', \tag{6.1}$$

where $\bar{u}_c'$, $\bar{w}_c'$ and $\bar{p}_c'$ are the velocity and pressure of the wave-induced current in the core, all of them of $O(1)$. The gauge functions $\mu_i(\epsilon), i = 1, 2$ are to be determined. In an infinitely long flume or unbounded sea, waves are damped out at $x \sim \infty$. The total steady-state discharge at any x must be equal to that of the pre-existing basic current,

$$\overline{\int_{-kh+kz_B}^{\eta} u\,\mathrm{d}z} = \overline{\int_{-kh+kz_B}^{\eta} (\bar{u}+\tilde{u})\,\mathrm{d}z} = \epsilon \int_{-kh+kz_B}^{0} \bar{u}_0\,\mathrm{d}z. \tag{6.2}$$

Taylor expansion of the middle integral of (6.2) for small η and substitution of (6.1) into the resulting equation yield

$$\mu_1(\epsilon) \int_{-kh+k\delta}^{0} \bar{u}_c'\,\mathrm{d}z + \overline{[\tilde{u}]_0 \tilde{\eta}} = O(\epsilon^3), \tag{6.3}$$

where $[\tilde{u}]_0$ denotes the orbital velocity at $z = 0$. The contribution of the BWBL has been ignored owing to the small thickness of $O(\epsilon^2)$.

It is evident that $\mu_1(\epsilon) = \epsilon^2$. After using the linear wave solutions for $\tilde{\eta}$ and $\tilde{u}$, the discharge condition (6.3) becomes

$$\int_{-kh+k\delta}^{0} \bar{u}_c'\,\mathrm{d}z = -\frac{AA^*}{2}\coth(kh). \tag{6.4}$$

As waves propagate in the positive x-direction, this term diminishes with x because of damping. Therefore the total flux of the Eulerian current,

$$\int_{-kh+kz_B}^{0} \bar{u}\,\mathrm{d}z = \int_{-kh+k\delta}^{0} \overline{(\epsilon\bar{u}_0 + \epsilon^2\bar{u}_c')}\,\mathrm{d}z + O(\epsilon^3),$$

must increase (decrease) its flux in the downstream direction for a wave-following (wave-opposing) current.

As a further inference, continuity requires

$$\epsilon^2\frac{\partial\bar{u}_c'}{\partial x} + \mu_2(\epsilon)\frac{\partial\bar{w}_c'}{\partial z} = 0. \tag{6.5}$$

Since $\partial\bar{u}_c'/\partial x = \epsilon^2\partial\bar{u}_c'/\partial x_2$ because of wave damping, we conclude that $\mu_2 = \epsilon^4$ so that (6.1) can be replaced by

$$\bar{u} = \epsilon\bar{u}_0 + \epsilon^2\bar{u}_c', \quad \bar{w} = \epsilon^4\bar{w}_c', \quad \bar{p} = \epsilon\bar{p}_0 + \epsilon^2\bar{p}_c'. \tag{6.6}$$

The presence of waves also modifies the friction velocity u_{fc} from that of the pure current, hence the value of α_c from α_0.

6.2. *Momentum balance of mean motion*

In the core region, the total Reynolds stresses (3.7) which appear on the right-hand sides of (3.17)–(3.18) can be approximated up to $O(\epsilon^4)$ by using the linear wave solutions (5.2), (5.3) and (5.4), and the basic current (4.4),

$$\bar{\tau}_{xx} = O(\epsilon^5), \quad \bar{\tau}_{zz} = O(\epsilon^5), \tag{6.7}$$

$$\begin{aligned}\bar{\tau}_{xz} &= \alpha_c\epsilon^2\bar{S}_c\left(\epsilon\frac{\partial\bar{u}_0}{\partial z} + \epsilon^2\frac{\partial\bar{u}_c'}{\partial z}\right) + \alpha_c\epsilon^2\hat{S}_c\overline{\tilde{\eta}\left(\frac{\partial\tilde{u}}{\partial z} + \frac{\partial\tilde{w}}{\partial x}\right)} + O(\epsilon^5)\\ &= \epsilon^4\left[\pm\frac{\alpha_0\alpha_c}{\kappa^2}\left(\frac{-z}{kh}\right) + \alpha_c\bar{S}_c\frac{\partial\bar{u}_c'}{\partial z} + \alpha_c AA^*\hat{S}_c\frac{\sinh(kh+z)}{\sinh(kh)}\right] + O(\epsilon^5).\end{aligned} \tag{6.8}$$

The period-averaged Reynolds stress $\bar{\tau}_{xz}$ can be written as the sum of the basic and perturbed parts

$$\bar{\tau}_{xz} = \pm\epsilon^4\frac{\alpha_0^2}{\kappa^2}\left(\frac{-z}{kh}\right) + \epsilon^4(\bar{\tau}_{xz}')_c. \tag{6.9}$$

The perturbed mean Reynolds stress is of order $O(\epsilon^4)$ with

$$(\bar{\tau}_{xz}')_c = \pm\frac{\alpha_0(\alpha_c - \alpha_0)}{\kappa^2}\left(\frac{-z}{kh}\right) + \alpha_c\bar{S}_c\frac{\partial\bar{u}_c'}{\partial z} + \alpha_c AA^*\hat{S}_c\frac{\sinh(kh+z)}{\sinh(kh)}. \tag{6.10}$$

Note that the mean turbulent shear stress $\alpha_c\bar{S}_c(\partial\bar{u}_c'/\partial z)$, associated directly with local eddy viscosity, is just a part of the perturbed Reynolds stress $(\bar{\tau}_{xz}')_c$, which includes also direct effects of wave fluctuations. The momentum equation (3.17) can now be approximated up to $O(\epsilon^4)$ by

$$\epsilon^2\frac{\partial}{\partial x_2}(\bar{E}_w + \epsilon^2\bar{p}_c') + \overline{\tilde{w}\tilde{\Omega}} = \epsilon^4\frac{\partial(\bar{\tau}_{xz}')_c}{\partial z} + O(\epsilon^5), \tag{6.11}$$

which governs the current shear in the core. Terms of the basic current disappear by cancellation.

To further simplify (6.11), we first note from the vertical momentum equation (3.18) that, upto $O(\epsilon^2)$,

$$\frac{\partial}{\partial z}(\bar{E}_w + \epsilon^2 \bar{p}'_c) = O(\epsilon^3) \tag{6.12}$$

Thus (6.11) can be written as

$$\epsilon^2 \frac{\partial}{\partial x_2}[\bar{E}_w + \epsilon^2 \bar{p}'_c]_0 + \overline{\widetilde{w}\widetilde{\Omega}} = \epsilon^4 \frac{\partial(\bar{\tau}'_{xz})_c}{\partial z} + O(\epsilon^5). \tag{6.13}$$

To complete the equation governing the mean shear stress, we shall calculate in the next subsection the vortex force term $\overline{\widetilde{w}\widetilde{\Omega}}$ up to $O(\epsilon^4)$.

6.3. *Vortex force* $\overline{\widetilde{w}\widetilde{\Omega}}$

Let us first find $\widetilde{\Omega}$ up to $O(\epsilon^3)$ from the oscillatory part of (3.13),

$$\frac{\partial \widetilde{\Omega}}{\partial t} + \bar{u}\frac{\partial \widetilde{\Omega}}{\partial x} + \bar{w}\frac{\partial \widetilde{\Omega}}{\partial z} + \widetilde{u}\frac{\partial \bar{\Omega}}{\partial x} + \widetilde{w}\frac{\partial \bar{\Omega}}{\partial z} + \widetilde{\widetilde{u}\frac{\partial \widetilde{\Omega}}{\partial x}} + \widetilde{\widetilde{w}\frac{\partial \widetilde{\Omega}}{\partial z}} = \widetilde{\Pi}. \tag{6.14}$$

$\widetilde{\Pi}$ is the oscillatory part of (3.14). From the definition (3.7), the oscillatory parts of the Reynolds stresses must be of $O(\epsilon^3)$,

$$\widetilde{\tau}_{xx} = 2\alpha_c \epsilon^2 \bar{S}_c \frac{\partial \widetilde{u}}{\partial x} + O(\epsilon^4), \quad \widetilde{\tau}_{zz} = 2\alpha_c \epsilon^2 \bar{S}_c \frac{\partial \widetilde{w}}{\partial z} + O(\epsilon^4), \tag{6.15}$$

$$\widetilde{\tau}_{xz} = \alpha_c \epsilon^2 \bar{S}_c \left(\frac{\partial \widetilde{u}}{\partial z} + \frac{\partial \widetilde{w}}{\partial x} \right) + O(\epsilon^4). \tag{6.16}$$

Using these results and the linear wave solutions in (3.14), we obtain

$$\widetilde{\Pi} = 2\epsilon^2 \alpha_c \frac{\partial^2 \bar{S}_c}{\partial z^2} \frac{\partial \widetilde{u}}{\partial z} + O(\epsilon^4). \tag{6.17}$$

For calculating $\overline{\widetilde{w}\widetilde{\Omega}}$ at $O(\epsilon^4)$, we shall only need the first harmonic component of $\widetilde{\Omega}$ at $O(\epsilon^3)$. Hence the last two terms on the left-hand side of (6.14) are of no concern. Using the fact that $\bar{w} = \bar{w}' = O(\epsilon^4)$, we obtain the governing equation for $\widetilde{\Omega}$ correct to $O(\epsilon^3)$

$$\frac{\partial \widetilde{\Omega}}{\partial t} + \bar{u}\frac{\partial \widetilde{\Omega}}{\partial x} + \widetilde{w}\frac{\partial \bar{\Omega}}{\partial z} = 2\epsilon^2 \alpha_c \frac{\partial^2 \bar{S}_c}{\partial z^2} \frac{\partial \widetilde{u}}{\partial z} + SHT + O(\epsilon^4), \tag{6.18}$$

where SHT represents the second harmonic terms. After integrating (6.18) with respect to t, we obtain

$$\widetilde{\Omega} = -\bar{u} \int \frac{\partial \widetilde{\Omega}}{\partial x}\, \mathrm{d}t - \frac{\partial \bar{\Omega}}{\partial z} \int \widetilde{w}\, \mathrm{d}t + 2\epsilon^2 \alpha_c \frac{\partial^2 \bar{S}_c}{\partial z^2} \int \frac{\partial \widetilde{u}}{\partial z}\, \mathrm{d}t + SHT + O(\epsilon^4). \tag{6.19}$$

Among all terms on the right-hand side, the second term dominates so that

$$\widetilde{\Omega} = -\frac{\partial \bar{\Omega}}{\partial z} \int \widetilde{w}\, \mathrm{d}t + O(\epsilon^3) = O(\epsilon^2). \tag{6.20}$$

Thus the vorticity fluctuation is due to the convection of the mean vorticity by vertical oscillations. However, this term is out of phase with $\widetilde{w}$, hence does not contribute to the vortex force. Note that the first term on the right-hand side of (6.19), which is of

$O(\epsilon^3)$, can be estimated by (6.20).

$$\bar{u}\int \frac{\partial \widetilde{\Omega}}{\partial x}\mathrm{d}t = -\bar{u}\frac{\partial \bar{\Omega}}{\partial z}\int\left(\int^t \frac{\partial \widetilde{w}}{\partial x}\mathrm{d}t'\right)\mathrm{d}t + O(\epsilon^4), \tag{6.21}$$

which is also out of phase with $\widetilde{w}$, hence does not affect the vortex force. Thus only the third term in (6.19) matters.

Finally, substituting (6.19) in $\overline{\widetilde{w}\widetilde{\Omega}}$, we find

$$\begin{aligned}\overline{\widetilde{w}\widetilde{\Omega}} &= 2\epsilon^2\alpha_c\frac{\partial^2\bar{S}_c}{\partial z^2}\overline{\widetilde{w}\int\frac{\partial\widetilde{u}}{\partial z}\mathrm{d}t} + O(\epsilon^4)\\ &= -\alpha_c\epsilon^4 AA^*\frac{\partial^2\bar{S}_c}{\partial z^2}\frac{\sinh^2(kh+z)}{\sinh^2(kh)} + O(\epsilon^5).\end{aligned} \tag{6.22}$$

It is interesting that the vortex force is related to the curvature of the eddy viscosity.

6.4. *Mean shear stress of wave-perturbed current*

With the vortex force calculated, let us return to the governing equation for the wave-perturbed mean motion in the core, (6.13)

$$\frac{\partial}{\partial x_2}[\bar{p}'_c + \epsilon^{-2}\bar{E}_w]_0 - \alpha_c AA^*\frac{\partial^2\bar{S}_c}{\partial z^2}\frac{\sinh^2(kh+z)}{\sinh^2(kh)} = \frac{\partial(\bar{\tau}'_{xz})_c}{\partial z}. \tag{6.23}$$

Integrating once with respect to z from $z=0$, we obtain

$$\begin{aligned}&z\frac{\partial}{\partial x_2}[\bar{p}'_c + \epsilon^{-2}\bar{E}_w]_0\\ &\quad= \alpha_c AA^*\frac{\partial^2\bar{S}_c}{\partial z^2}\left(\frac{\sinh(2(kh+z)) - \sinh(2kh) - 2z}{4\sinh^2(kh)}\right) + (\tau'_{xz})_c - [(\bar{\tau}'_{xz})_c]_0,\end{aligned} \tag{6.24}$$

where $\partial^2\bar{S}_c/\partial z^2 = -2/kh = \text{constant}$ has been used.

The wave-induced pressure gradient can be expressed in terms of the wave-induced mean shear $[(\bar{\tau}'_{xz})_c]_+$, at the top edge of the BWBL. By setting $z = -kh + k\delta$ in (6.24), we have

$$\begin{aligned}&\frac{\partial}{\partial x_2}[\bar{p}'_c + \epsilon^{-2}\bar{E}_w]_0\\ &\quad= \frac{-1}{kh}\left\{\alpha_c AA^*\frac{\partial^2\bar{S}_c}{\partial z^2}\left(\frac{-\sinh(2kh)+2kh}{4\sinh^2(kh)}\right) + [(\bar{\tau}'_{xz})_c]_+ - [(\bar{\tau}'_{xz})_c]_0\right\}.\end{aligned} \tag{6.25}$$

This result can be used in (6.24) to eliminate the pressure gradient. On the other hand, we have from (6.10),

$$\frac{z}{kh}[(\bar{\tau}'_{xz})_c]_+ + (\bar{\tau}'_{xz})_c = \frac{z}{kh}\alpha_c\left[\bar{S}_c\frac{\partial\bar{u}'_c}{\partial z}\right]_+ + \alpha_c\bar{S}_c\frac{\partial\bar{u}'_c}{\partial z} + \alpha_c AA^*\hat{S}_c\frac{\sinh(kh+z)}{\sinh(kh)}.$$

It then follows that (6.24) can be written as

$$\begin{aligned}&\alpha_c AA^*\frac{\partial^2\bar{S}_c}{\partial z^2}\frac{(kh+z)\sinh(2kh) - kh\sinh(2(kh+z))}{4kh\sinh^2(kh)} + \left(1+\frac{z}{kh}\right)[(\bar{\tau}'_{xz})_c]_0\\ &\qquad= \alpha_c\frac{z}{kh}\left[\bar{S}_c\frac{\partial\bar{u}'_c}{\partial z}\right]_+ + \alpha_c\bar{S}_c\frac{\partial\bar{u}'_c}{\partial z} + \alpha_c AA^*\hat{S}_c\frac{\sinh(kh+z)}{\sinh(kh)}.\end{aligned} \tag{6.26}$$

Next, we recall the definition of u_{fc} and its dimensionless equivalent α_c

$$\alpha_c^2 = \pm\kappa^2\epsilon^{-4}[\bar{\tau}_{xz}]_+. \tag{6.27}$$

Making use of (6.8) in (6.27), we have

$$\alpha_c = \pm\kappa^2\epsilon^{-1}\left[\bar{S}_c\frac{\partial\bar{u}_0}{\partial z}\right]_+ \pm\kappa^2\left[\bar{S}_c\frac{\partial\bar{u}_c'}{\partial z}\right]_+ + O(\epsilon) = \alpha_0 \pm \kappa^2\left[\bar{S}_c\frac{\partial\bar{u}_c'}{\partial z}\right]_+, \tag{6.28}$$

where (4.4) has been used in the last step. We obtain by definition, the expected result

$$\alpha_c - \alpha_0 = \pm\kappa^2\left[\bar{S}_c\frac{\partial\bar{u}_c'}{\partial z}\right]_+. \tag{6.29}$$

Finally, the perturbed turbulent shear stress in the core is obtained,

$$\begin{aligned}\alpha_c\bar{S}_c\frac{\partial\bar{u}_c'}{\partial z} &= \alpha_c AA^*\frac{\partial^2\bar{S}_c}{\partial z^2}\frac{(kh+z)\sinh(2kh) - kh\sinh(2(kh+z))}{4kh\sinh^2(kh)} \\ &+ \left(1+\frac{z}{kh}\right)[(\bar{\tau}_{xz}')_c]_0 \pm \frac{\alpha_c(\alpha_c-\alpha_0)}{\kappa^2}\left(\frac{-z}{kh}\right) - \alpha_c AA^*\hat{S}_c\frac{\sinh(kh+z)}{\sinh(kh)}.\end{aligned} \tag{6.30}$$

This result will be integrated later to obtain the wave-perturbed current $\bar{u}_c'$. Clearly, two boundary values are needed: the velocity $\bar{u}_c'$ at the upper edge of the bed boundary layer and the mean shear stress $[(\bar{\tau}_{xz}')_c]_0$ on the mean free surface. For the former, we must analyse the wave-perturbed mean motion inside the bed boundary layer.

7. Bed boundary layer

A unified treatment can be given for cases A and B. Recalling that $k\delta = O(\epsilon^2)$, an inner depth variable Z will be defined by

$$Z = \frac{z+kh}{\alpha_b\epsilon^2}. \tag{7.1}$$

For case A, we need only set $\alpha_b = \alpha_c$. Let us first estimate the orders of magnitude of the vertical velocities, both mean and oscillatory, in the bed boundary layer. The horizontal velocities and dynamic pressures are more obvious. Let us express the mean and oscillatory flow fields as follows.

$$\bar{u} = \epsilon\bar{u}_0 + \epsilon^2\bar{u}_b', \quad \bar{w} = \sigma_1(\epsilon)\bar{w}_b' + \cdots, \quad \bar{p} = \epsilon\bar{p}_0 + \epsilon^2\bar{p}_b', \tag{7.2}$$

$$\tilde{u} = \epsilon\tilde{u}_b, \quad \tilde{w} = \sigma_2(\epsilon)\tilde{w}_b, \quad \tilde{p} = \epsilon\tilde{p}_b, \tag{7.3}$$

where the gauge functions $\sigma_1(\epsilon)$ and $\sigma_2(\epsilon)$ are to be determined. From the time-averaged continuity equation,

$$\epsilon^4\frac{\partial\bar{u}_b'}{\partial x_2} + \frac{\sigma_1(\epsilon)}{\alpha_b\epsilon^2}\frac{\partial\bar{w}_b'}{\partial Z} = 0. \tag{7.4}$$

Clearly $\sigma_1 = O(\epsilon^6)$ so that we can write $\bar{w} = \epsilon^6\bar{w}_b' = O(\epsilon^6)$.

To find the order of the oscillatory motion inside the boundary layer, we invoke the continuity equation,

$$\epsilon\frac{\partial\tilde{u}_b}{\partial x} + \epsilon^3\frac{\partial\tilde{u}_b}{\partial x_2} + \frac{\sigma_2(\epsilon)}{\alpha_b\epsilon^2}\frac{\partial\tilde{w}_b}{\partial Z} = 0, \tag{7.5}$$

hence $\sigma_2 = O(\epsilon^3)$. It follows from (7.5) that

$$\tilde{w}_b' = -\alpha_b \int_{Z_B}^{Z} \frac{\partial \tilde{u}_b}{\partial x}\, \mathrm{d}Z + O(\epsilon) \quad \text{with} \quad Z_B = \frac{k z_B}{\alpha_b \epsilon^2}. \tag{7.6}$$

With these estimates, we can now simplify the mean horizontal momentum equation in order to show just what is needed from the oscillatory motion. Explicit calculations of the required oscillatory motion will then be worked out, and finally the horizontal component of wave-perturbed current velocity will be found.

7.1. *Approximate momentum balance of the mean motion*

Substituting (7.2) and (7.3) into (3.7), we obtain the total Reynolds stress inside the boundary layer

$$\bar{\tau}_{xx} = 2\epsilon^8 \alpha_b^2 Z \frac{\partial \bar{u}_b'}{\partial x_2}, \quad \bar{\tau}_{zz} = 2\epsilon^8 \alpha_b Z \frac{\partial \bar{w}_b'}{\partial Z}, \quad \bar{\tau}_{xz} = \pm\epsilon^4 \frac{\alpha_0^2}{\kappa^2} + \epsilon^4 (\bar{\tau}_{xz}')_b. \tag{7.7}$$

In the equation for $\bar{\tau}_{xz}$, where the first term on the right-hand side is the shear stress of the basic current, and the second is the wave-induced mean shear $(\bar{\tau}_{xz}')_b$, given by

$$(\bar{\tau}_{xz}')_b = \alpha_b Z \frac{\partial \bar{u}_b'}{\partial Z} + \epsilon^{-2}(\alpha_b - \alpha_0) S_b \frac{\partial \bar{u}_0}{\partial z} = \alpha_b Z \frac{\partial \bar{u}_b'}{\partial Z} \pm (\alpha_b - \alpha_0)\frac{\alpha_0}{\kappa^2}, \tag{7.8}$$

the last term above has been simplified by using (4.4). After substituting (7.2), (7.3) and (7.7) into the horizontal mean momentum equation (3.17), we obtain,

$$\frac{\partial \overline{\tilde{u}_b \tilde{w}_b}}{\partial Z} = \frac{\partial (\bar{\tau}_{xz}')_b}{\partial Z} + O(\epsilon). \tag{7.9}$$

Integrating this with respect to Z from the upper edge of the boundary layer,

$$Z = Z_\delta \equiv \frac{k\delta}{\alpha_b \epsilon^2}, \tag{7.10}$$

we obtain

$$\overline{\tilde{u}_b \tilde{w}_b} - [\overline{\tilde{u}_b \tilde{w}_b}]_+ = (\bar{\tau}_{xz}')_b - [(\bar{\tau}_{xz}')_b]_+ = (\bar{\tau}_{xz}')_b - [(\bar{\tau}_{xz}')_c]_+. \tag{7.11}$$

The last equality follows by the continuity of stress at the top edge of the BWBL, signified by the subscript $[\cdots]_+$. Physically, (7.9) or (7.11) states that the total mean shear stress is not constant across the bed boundary layer†. Second-order mean shear is forced by the Reynolds stress due directly to oscillations in the boundary layer, which should be distinguished from Reynolds stress due to turbulent fluctuations. This result is similar to that of Eulerian streaming in a oscillatory laminar boundary layer of Stokes.

By using (6.10), (7.8) and then (6.29), the right-hand side of (7.11) can be written as

$$(\bar{\tau}_{xz}')_b - [(\bar{\tau}_{xz}')_c]_+ = \alpha_b Z \frac{\partial \bar{u}_b'}{\partial Z} \pm \frac{\alpha_0 \alpha_b - \alpha_c^2}{\kappa^2} + O(\epsilon). \tag{7.12}$$

It then follows from (7.8), (7.11) and (7.12) that

$$Z \frac{\partial \bar{u}_b'}{\partial Z} = \frac{\overline{\tilde{u}_b \tilde{w}_b}}{\alpha_b} - \left(\pm \frac{\alpha_0 \alpha_b - \alpha_c^2}{\alpha_b \kappa^2} + \frac{[\overline{\tilde{u}_b \tilde{w}_b}]_+}{\alpha_b} \right) + O(\epsilon), \tag{7.13}$$

† In the theory by Grant & Madsen (1979, 1986), the oscillation-induced Reynolds stress was not accounted for, therefore their current profile remains logarithmic in height even with waves.

which can be integrated from $Z = Z_B$, to give the wave-perturbed current in the bed boundary layer

$$\bar{u}_b'(Z) = \int_{Z_B}^{Z} \frac{\overline{\widetilde{u}_b \widetilde{w}_b}}{\alpha_b Z} \mathrm{d}Z - \left(\pm \frac{\alpha_0 \alpha_b - \alpha_c^2}{\alpha_b \kappa^2} + \frac{[\overline{\widetilde{u}_b \widetilde{w}_b}]_+}{\alpha_b} \right) \ln\left(\frac{Z}{Z_B}\right) + O(\epsilon). \quad (7.14)$$

Its value at the upper edge of the BWBL ($Z = Z_\delta$) gives the lower boundary condition for $\bar{u}_c'$

$$[\bar{u}_c']_+ = \int_{Z_B}^{Z_\delta} \frac{\overline{\widetilde{u}_b \widetilde{w}_b}}{\alpha_b Z} \mathrm{d}Z - \left(\pm \frac{\alpha_0 \alpha_b - \alpha_c^2}{\alpha_b \kappa^2} + \frac{[\overline{\widetilde{u}_b \widetilde{w}_b}]_+}{\alpha_b} \right) \ln\left(\frac{Z_\delta}{Z_B}\right) + O(\epsilon), \quad (7.15)$$

which holds for both cases A and B. In case A, we need only set $\alpha_c = \alpha_b$. In (7.15) the wave-Reynolds stress is to be determined in the next section after solving the oscillatory motion inside the BWBL. Note that $[\bar{u}_c']_+$ depends implicitly on α_c and α_b which are yet to be found.

7.2. *Oscillatory motion:* $\widetilde{u}_b$

Making use of (7.6), the wave-induced Reynolds stress in (7.13) can be expressed as

$$\overline{\widetilde{u}_b \widetilde{w}_b} = -\alpha_b \widetilde{u}_b \overline{\int_{Z_B}^{Z} \frac{\partial \widetilde{u}_b}{\partial x} \mathrm{d}Z} + O(\epsilon). \quad (7.16)$$

The oscillatory flow $\widetilde{u}_b$ is required only to the leading order in order to integrate (7.14) for $\bar{u}_b'$. After using (7.3) and (7.6), and the oscillatory parts of the Reynolds stress (3.7), the boundary-value problem for the oscillatory motion is that of the Stokes problem with a depth-linear eddy viscosity. The solution has been given by Kajiura (1968)

$$\widetilde{u}_b = \frac{A}{2\sinh(kh)} (1 - K(Z)) \, \mathrm{e}^{\mathrm{i}\theta} + \text{c.c.} \quad \text{where} \quad K(Z) = \frac{K_0(2\sqrt{Z}\mathrm{e}^{-\mathrm{i}\pi/4})}{K_0(2\sqrt{Z_B}\mathrm{e}^{-\mathrm{i}\pi/4})}, \quad (7.17)$$

with K_0 being the Kelvin function of the zeroth order. We now follow Grant & Madsen (1979) and define the outer edge of the bottom wave boundary layer Z_δ by the condition $|\widetilde{u}_b / [\widetilde{u}_b]_+| = 0.95$† or from (7.17)

$$|K(Z_\delta)| = 0.05. \quad (7.18)$$

Now the wave-induced Reynolds stress (7.16) can be calculated from (7.17)

$$\overline{\widetilde{u}_b \widetilde{w}_b}(Z) = -\frac{\alpha_b A A^*}{4\sinh^2(kh)} \left[(1 - K^*) \int_{Z_B}^{Z} \mathrm{i}(1 - K) \, \mathrm{d}Z + \text{c.c.} \right] + O(\epsilon). \quad (7.19)$$

At the upper edge of the boundary layer, $K \to 0$, thus,

$$[\overline{\widetilde{u}_b \widetilde{w}_b}]_+ = -\frac{\alpha_b A A^*}{2\sinh^2(kh)} \int_{Z_B}^{Z_\delta} \mathrm{Im}(K) \, \mathrm{d}Z + O(\epsilon). \quad (7.20)$$

8. Wave damping rate

After finding the oscillatory flow field (7.17) inside the bed boundary layer, we can now calculate the rate of wave damping explicitly. In view of (7.3) and (7.6), the first

† We have checked for case A, that this numerical value is immaterial as long as it is close to 1.

integral on the left-hand side of the mechanical energy equation (5.5) representing dissipation inside the bed boundary layer can be approximated as follows

$$\int_{Z_B}^{Z_\delta} Z\overline{\left(\frac{\partial \tilde{u}_b}{\partial Z}\right)^2}\,\mathrm{d}z = \frac{\alpha_b A A^*}{2\sinh^2(kh)}\int_{Z_B}^{\infty} Z\frac{\partial K(Z)}{\partial Z}\left(\frac{\partial K(Z)}{\partial Z}\right)^*\mathrm{d}z. \tag{8.1}$$

The integral on the right-hand side can be evaluated numerically. The second term in (5.5) which represents energy dissipation in the core, can be easily calculated from the linear wave solution

$$\epsilon^2\frac{1}{2}\int_{-kh+k\delta}^{0}\alpha_c\bar{S}_c\overline{\left(\frac{\partial \tilde{u}_i}{\partial x_j}+\frac{\partial \tilde{u}_j}{\partial x_i}\right)^2}\,\mathrm{d}z = \epsilon^4\alpha_c A A^*\frac{2kh\cosh^2(kh)-\sinh(2kh)}{2kh\sinh^2(kh)}, \tag{8.2}$$

where (3.8) has been used for $\bar{S}_c$ and terms smaller by the factor of $k\delta = O(\epsilon^2)$ have been ignored. Similarly, the rate of pressure working on the right-hand side of (5.5) can also be evaluated

$$-\frac{\partial}{\partial x}\int_{-kh+kz_B}^{0}\overline{\tilde{u}\tilde{p}}\;\mathrm{d}z \approx -\left(\frac{\sinh(2kh)+2kh}{8\sinh^2(kh)}\right)\frac{\partial A A^*}{\partial x_2}. \tag{8.3}$$

Summarizing (5.5) and (8.1)–(8.3), we have

$$\frac{\partial A A^*}{\partial x_2} = -\beta A A^*, \tag{8.4}$$

where

$$\beta = \alpha_c\beta_c + \alpha_b\beta_b, \tag{8.5}$$

$$\beta_c = 4\frac{2kh\cosh^2(kh)-\sinh(2kh)}{kh\,(\sinh(2kh)+2kh)}, \tag{8.6}$$

$$\beta_b = \frac{2AA^*}{\sinh(2kh)+2kh}\int_{Z_B}^{\infty} Z\frac{\partial K(Z)}{\partial Z}\left(\frac{\partial K(Z)}{\partial Z}\right)^*\mathrm{d}z, \tag{8.7}$$

with β_c and β_b representing contributions from the core and the bed boundary-layer, respectively.

Since the damping rate affects the evolution over distances much longer than both the wave length and the roughness size, local inaccuracies due to boundary-layer approximation may not be crucial. Hence, the results here may even apply for a rough bed with large and/or well-separated roughness elements (case C). This will be checked later.

9. Perturbed Reynolds stress on the still water surface

Near the free surface, a wave boundary layer also exists in principle. Because of the stress-free condition, this boundary layer is weak. In Appendix B it is shown that, to the desired accuracy, the boundary-layer corrections can be ignored in calculating the current. We shall therefore use only the outer solution to derive an approximate surface boundary condition for the mean current at the mean water level. Our approach is to integrate the governing equations from the moving surface down to the still water surface at $z = 0$, invoke the surface boundary conditions, and then approximate the time-averaged results to the desired accuracy. This approach has been employed before by Liu & Davis (1977) in their study of wave-induced current, and is essentially the same as that in the theory of radiation stresses arising in the

depth-integrated and time-averaged momentum balance of a wave field (see, e.g. Phillips 1977; Mei 1989).

By integrating the horizontal momentum equation from $z = 0$ to the instantaneous sea level, applying the boundary conditions, and taking the time averages, we obtain the following exact result,

$$[\bar{\tau}_{xz}]_0 - [\overline{uw}]_0 = -\frac{\partial}{\partial x}\overline{\int_0^\eta (uu + P - \tau_{xx})\,\mathrm{d}z}. \tag{9.1}$$

On $z = 0$, the basic current $\bar{u}_0$ has zero shear stress. It follows from (6.8) that the leading term is the result of wave disturbance, i.e. $[\bar{\tau}_{xz}]_0 = \epsilon^4[\bar{\tau}'_{xz}]_0$. Up to $O(\epsilon^4)$, not only the wave boundary-layer corrections can be ignored, but the right-hand side of (9.1) can be approximated so that

$$\epsilon^4[\bar{\tau}'_{xz}]_0 = [\overline{uw}]_0 - \frac{\partial}{\partial x}\overline{\int_0^\eta P\,\mathrm{d}z} + O(\epsilon^5). \tag{9.2}$$

On the right-hand side, the first term represents the averaged wave-induced momentum flux (wave-induced Reynolds stress) while the second is the averaged net pressure force in the horizontal direction; their sum makes up the mean shear stress at the mean sea level. We now calculate these two terms.

From the definition of the dynamic pressure, $p = P + (gk/\omega^2)z$, we obtain

$$\frac{\partial}{\partial x}\overline{\int_0^\eta P\,\mathrm{d}z} = \epsilon^2\frac{\partial}{\partial x_2}(\overline{[p]_0\eta}) - \epsilon^2\frac{\partial}{\partial x_2}\left(\overline{\frac{\eta^2}{2}}\frac{gk}{\omega^2}\right) + O(\epsilon^5). \tag{9.3}$$

Making use of the linear wave solutions on the right-hand side, we obtain

$$\frac{\partial}{\partial x}\overline{\int_0^\eta P\,\mathrm{d}z} = \epsilon^4\frac{\coth(kh)}{4}\frac{\partial AA^*}{\partial x_2} + O(\epsilon^5). \tag{9.4}$$

Clearly, this variation owes its existence to wave attenuation.

Next we compute the wave-induced Reynolds stress on the mean surface, $[\overline{uw}]_0$. For this we turn to the core and recall the following identity

$$\frac{\partial u^2}{\partial x} + \frac{\partial uw}{\partial z} = \frac{\partial E}{\partial x} + w\Omega. \tag{9.5}$$

Since $\bar{u} = \epsilon\bar{u}_0 + \epsilon^2\bar{u}'$, $\partial\bar{f}/\partial x_2 = O(\epsilon^2 f)$, and $\bar{w} = O(\epsilon^3)$, we have

$$\frac{\partial\overline{uw}}{\partial z} = \frac{\partial\overline{\tilde{u}\tilde{w}}}{\partial z} + O(\epsilon^5) = \epsilon^2\frac{1}{2}\frac{\partial}{\partial x_2}(\overline{\tilde{w}^2} - \overline{\tilde{u}^2}) + \overline{\tilde{w}\tilde{\Omega}} + O(\epsilon^5). \tag{9.6}$$

Making use of (6.22) for $\overline{\tilde{w}\tilde{\Omega}}$ and the linear wave solutions in (9.6), we obtain

$$\frac{\partial\overline{\tilde{u}\tilde{w}}}{\partial z} = -\alpha_c\epsilon^4 AA^*\frac{\partial^2\bar{S}_c}{\partial z^2}\frac{\sinh^2(kh+z)}{\sinh^2(kh)} - \frac{\epsilon^4}{4\sinh^2(kh)}\frac{\partial AA^*}{\partial x_2} + O(\epsilon^5).$$

This equation can be integrated from the upper edge of the bottom boundary layer to give

$$\overline{\tilde{u}\tilde{w}}(z) = [\overline{\tilde{u}\tilde{w}}]_+ - \alpha_c\epsilon^4 AA^*\frac{\partial^2\bar{S}_c}{\partial z^2}\frac{\sinh(2(kh+z)) - 2(kh+z)}{4\sinh^2(kh)} - \frac{\epsilon^4(kh+z)}{4\sinh^2(kh)}\frac{\partial AA^*}{\partial x_2} + O(\epsilon^5), \quad kh + z > k\delta. \tag{9.7}$$

Because of (7.3), the first term on the right-hand side can be matched to the boundary-layer solution given by (7.20),

$$[\overline{\tilde{u}\tilde{w}}]_+ = \epsilon^4[\overline{\tilde{u}_b\tilde{w}_b}]_+ = -\epsilon^4\frac{\alpha_b\,AA^*}{2\sinh^2(kh)}\int_{Z_B}^{Z_\delta}\mathrm{Im}(K)\,\mathrm{d}z, \tag{9.8}$$

where $Z_\delta = \delta/(\alpha_b\epsilon^2)$. Substituting this result in (9.7), we obtain

$$\begin{aligned}\overline{\tilde{u}\tilde{w}} &= -\epsilon^4\frac{\alpha_b\,AA^*}{2\sinh^2(kh)}\int_{Z_B}^{Z_\delta}\mathrm{Im}(K)\,\mathrm{d}z - \frac{\epsilon^4(kh+z)}{4\sinh^2(kh)}\frac{\partial AA^*}{\partial x_2}\\ &\quad -\alpha_c\epsilon^4 AA^*\frac{\partial^2\bar{S}_c}{\partial z^2}\frac{\sinh(2(kh+z))-2(kh+z)}{4\sinh^2(kh)} + O(\epsilon^5), \quad kh+z > k\delta,\end{aligned} \tag{9.9}$$

for all z in the core. In particular, its value at $z = 0$ is

$$\begin{aligned}[\overline{\tilde{u}\tilde{w}}]_0 &= -\epsilon^4\frac{\alpha_b\,AA^*}{2\sinh^2(kh)}\int_{Z_B}^{Z_\delta}\mathrm{Im}(K)\,\mathrm{d}z - \frac{\epsilon^4 kh}{4\sinh^2(kh)}\frac{\partial AA^*}{\partial x_2}\\ &\quad -\alpha_b\epsilon^4 AA^*\frac{\partial^2\bar{S}_c}{\partial z^2}\frac{\sinh(2kh)-2kh}{4\sinh^2(kh)} + O(\epsilon^5).\end{aligned} \tag{9.10}$$

The shear stress at the mean sea level then follows by combining (9.4) and (9.10) with (9.2)

$$\begin{aligned}[\bar{\tau}'_{xz}]_0 &= -\frac{\alpha_b AA^*}{2\sinh^2(kh)}\int_{Z_B}^{Z_\delta}\mathrm{Im}(K)\,\mathrm{d}z - \left(\frac{\coth(kh)}{4} + \frac{kh}{4\sinh^2(kh)}\right)\frac{\partial AA^*}{\partial x_2}\\ &\quad -\alpha_c AA^*\frac{\partial^2\bar{S}_c}{\partial z^2}\frac{\sinh(2kh)-2kh}{4\sinh^2(kh)}.\end{aligned} \tag{9.11}$$

This boundary value completes the perturbed turbulent stress (6.31) in the core, and is a key result of this work. Physically, despite the absence of wind, the perturbed Reynolds stress is not zero on $z = 0$, owing to the combined effects of the wave-induced Reynolds stress at the bottom, wave damping and the curvature of the eddy viscosity. There is a simpler result in the theory for deep-water waves, where molecular viscosity gives rise to a finite shear stress on the mean surface due to wave damping (Phillips 1977).

10. Final solution for the core

10.1. *Formulae for mean turbulent stress and current velocity*

With the surface boundary condition (9.11), the perturbed turbulent stress follows from (6.30), which can be rearranged as

$$\begin{aligned}\bar{S}_c\frac{\partial\bar{u}'_c}{\partial z} &= -\underbrace{AA^*\hat{S}_c\frac{\sinh(kh+z)}{\sinh(kh)}}_{\tau_{\hat{S}}} \pm \underbrace{\frac{(\alpha_c-\alpha_0)}{\kappa^2}\left(\frac{-z}{kh}\right)}_{\tau_{\alpha_c}} + \underbrace{\frac{\beta AA^*}{\alpha_c}\frac{(z+kh)\,(2kh+\sinh(2kh))}{8kh\sinh^2(kh)}}_{\tau_\beta}\\ &\quad -\underbrace{\frac{\alpha_b}{\alpha_c}\frac{AA^*(kh+z)}{2kh\sinh^2(kh)}\int_{Z_B}^{Z_\delta}\mathrm{Im}(K)\mathrm{d}z}_{\tau_B} - \underbrace{AA^*\frac{\partial^2\bar{S}_c}{\partial z^2}\frac{\sinh(2(kh+z))-2(kh+z)}{4\sinh^2(kh)}}_{\tau_{\bar{S}''}},\end{aligned} \tag{10.1}$$

where (8.4) for the wave damping rate has been used.

As labelled above, the perturbed turbulent stress $\bar{S}_c(\partial \bar{u}_c'/\partial z)$ is the sum of the following parts:

$\tau_{\hat{S}}$: Surface distortion of the eddy viscosity, which is always negative and greatest on $z = 0$.

τ_{α_c}: Wave-induced change of friction velocity, where the upper (lower) sign corresponds to wave-following (-opposing) current.

τ_β: Wave damping, which is always positive.

τ_B: Wave-induced Reynolds stress from the bottom boundary layer, which is always negative.

$\tau_{\bar{S}''}$: Curvature of the eddy viscosity, which originates from the vortex force (cf. (6.22)) and is always positive.

A negative stress should lead to reduction (increase) of surface current velocity if waves and current are in the same (opposite) direction. The opposite, of course, holds for a positive stress. The magnitude of each term will be examined later to find the net consequence. Upon integration from the outer edge of the wave boundary layer, we obtain the wave-perturbed current velocity $\bar{u}_c'$

$$\begin{aligned}\bar{u}_c'(z) = [\bar{u}_c']_+ &- AA^* \int_{-kh+\delta}^{z} \frac{\sinh(kh+z')}{(-z')\sinh(kh)}\,\mathrm{d}z' \pm \frac{\alpha_c - \alpha_0}{\kappa^2}\ln\left(\frac{kh+z}{\delta}\right)\\ &- \frac{\beta AA^*}{\alpha_c}\left(\frac{(2kh+\sinh(2kh))}{8\sinh^2(kh)}\right)\ln\left(\frac{-z}{kh-\delta}\right)\\ &+ \left(\frac{\alpha_b}{\alpha_c}\frac{AA^*}{2\sinh^2(kh)}\int_{Z_B}^{Z_\delta}\mathrm{Im}(K(Z))\,\mathrm{d}z\right)\ln\left(\frac{-z}{kh-\delta}\right)\\ &- AA^*\frac{\partial^2 \bar{S}_c}{\partial z^2}\int_{-kh+\delta}^{z}\left(\frac{\sinh(2(kh+z')-2(kh+z')}{4\bar{S}_c\sinh^2(kh)}\right)\mathrm{d}z',\end{aligned} \tag{10.2}$$

where $[\bar{u}_c']_+$ is given by (7.15). The final current velocity in the core is $\bar{u} = \epsilon\bar{u}_0 + \epsilon^2\bar{u}_c'$ by summing (2.13) and (10.2). Note that $\bar{u}_c'$ depends on two parameters α_c and α_b, which remain to be determined. For a smooth bed (case A), we simply set $\alpha_c = \alpha_b$.

10.2. *Friction velocities*

For a smooth bed (case A), the friction velocity u_{fc} or its dimensionless equivalent α_c is determined by requiring the constancy of discharge (6.3).

For a rough bed (case B), $\alpha_b \neq \alpha_c$; we must further invoke the scheme of Grant & Madsen. To facilitate comparison, we begin with the dimensional form of the friction velocity inside the bottom boundary layer. The total friction velocity u_{fb} is defined by the magnitude of the total bottom shear stress

$$\rho u_{fb}^2 = \max([\tau_{xz}^*]_B), \tag{10.3}$$

where $[\ ]_B$ represents a quantity evaluated at the bottom $z^* = -h + z_B$ in physical coordinates, or $z = -kh + kz_B$ in dimensionless coordinates.

By requiring that waves and current assume the same eddy viscosity ν_b, (2.10), the Reynolds stress $[\tau_{xz}^*]_B$ can be written as

$$[\tau_{xz}^*]_B = \rho\kappa\, u_{fb}\left[(h+z^*)\frac{\partial \bar{u}^*}{\partial z^*} + (h+z^*)\frac{\partial \widetilde{u}^*}{\partial z^*}\right]_B, \tag{10.4}$$

where terms smaller than that retained by a factor of $k\delta$ have been ignored. In view of the definition of u_{fb}, (10.3), it follows from (10.4) that

$$u_{fb} = \kappa \max \left[(h+z^*)\frac{\partial \bar{u}^*}{\partial z^*} + (h+z^*)\frac{\partial \tilde{u}^*}{\partial z^*} \right]_B . \tag{10.5}$$

After normalizing u_{fb} by $C\epsilon^2$, and substituting (6.1) and (7.3) in (10.5), we obtain

$$\alpha_b = \kappa^2 \max \left[\frac{kh+z}{\epsilon} \left(\frac{\partial \bar{u}_0}{\partial z} \right) + Z \left(\frac{\partial \bar{u}_b'}{\partial Z} \right) + \frac{Z}{\epsilon} \frac{\partial \tilde{u}_b}{\partial Z} \right]_B + O(\epsilon). \tag{10.6}$$

In accordance with (4.4), the first term in the brackets in (10.6) is just $\pm\alpha_0/\kappa^2$. From the governing equation of the mean current inside the bed boundary layer, (7.13), the second term in the brackets of (10.6) is

$$\left[Z \frac{\partial \bar{u}_b'}{\partial Z} \right]_B = -\left(\pm \frac{\alpha_0 \alpha_b - \alpha_c^2}{\alpha_b \kappa^2} + \frac{[\overline{\tilde{u}_b \tilde{w}_b}]_+}{\alpha_b} \right) + O(\epsilon), \tag{10.7}$$

where $[\overline{\tilde{u}_b \tilde{w}_b}]_+$ is given by (7.20). Use has been made of the fact that the wave-induced Reynolds stress vanishes on the seabed. Lastly, the wave solution inside the bed boundary layer, (7.17), gives the third term

$$\left[\frac{-A}{2\sinh(kh)} \left(Z \frac{\partial K}{\partial Z} e^{i\theta} + \text{c.c.} \right) \right]_B . \tag{10.8}$$

For small Z_B, as in many field cases, we can approximate the Kelvin function (Abramowitz & Stegun 1972) to obtain

$$\left[Z \frac{\partial K}{\partial Z} \right]_B = \frac{1}{2\ln\left(\frac{1-i}{\sqrt{2}}\right) + \ln(Z_B) + 2\gamma} + O(Z_B), \tag{10.9}$$

where $\gamma = 0.57722$. Therefore, for sufficiently small Z_B, (10.8) is practically of order $O(\epsilon)$ and all terms on the right-hand side of (10.6) are of order unity.

For any complex number $a = |a| e^{i\Theta}$, where Θ is the phase of a, the following is an identity,

$$\max[a e^{i\theta} + \text{c.c.}] = \max\left[|a| e^{i(\theta+\Theta)} + \text{c.c.} \right] = 2|a| . \tag{10.10}$$

With this, (10.6) can be reduced to

$$\begin{aligned} \alpha_b &= \kappa^2 \left| \pm\frac{\alpha_0}{\kappa^2} - \left(\pm \frac{\alpha_0 \alpha_b - \alpha_c^2}{\alpha_b \kappa^2} + \frac{[\overline{\tilde{u}_b \tilde{w}_b}]_+}{\alpha_b} \right) \right| + \frac{\kappa^2}{\epsilon} \left| \frac{A}{\sinh(kh)} \left(Z \frac{\partial K}{\partial Z} \right) \right|_B \\ &= \kappa^2 \left| \frac{\pm\alpha_c^2}{\alpha_b \kappa^2} + \frac{[\overline{\tilde{u}_b \tilde{w}_b}]_+}{\alpha_b} \right| + \frac{\kappa^2}{\epsilon} \left| \frac{A}{\sinh(kh)} \left(Z \frac{\partial K}{\partial Z} \right) \right|_B . \end{aligned} \tag{10.11}$$

This implicit relation between α_b and α_c reduces to that of Grant & Madsen only if we disregard the wave-induced Reynolds stress $[\overline{\tilde{u}_b \tilde{w}_b}]_+$ which is important here.

10.3. *Numerical procedure*

In water of given depth h, we suppose that the basic current and the wave parameters are known in advance.

For a steady current, the bottom roughness z_B is usually determined by fitting the logarithmic profile with the measured profile of the pure current. Based on experiments Mathisen& Madsen (1996*a*, *b*) have shown that the same value can be taken if waves are also present.

Authors	Roughness	Λ_k	Δ_k	$Re_w(10^4)$	a_b/k_N	Bed conditions
Bakker & Doorn (1978)	Rectangular	15	2	$1.9 \sim 2.8$	$3.35 \sim 4.11$	C
Kemp & Simons (1982)	Smooth bed	0	0	$0.07 \sim 0.36$	∞	A
Kemp & Simons (1982)	Triangular	18	5	$0.07 \sim 0.36$	$0.94 \sim 1.76$	C
Kemp & Simons (1983)	Triangular	18	5	$0.07 \sim 036$	$0.94 \sim 1.76$	C
Mathisen & Madsen (1996*a*)	Triangular	100	15	$0.5 \sim 1.6$	$0.2 \sim 0.44$	C
Mathisen & Madsen (1996*b*)	Triangular	200	15	$0.5 \sim 1.8$	$1.14 \sim 1.74$	C
Klopman (1994)	Sand	2	2	1.1	4.25	C

TABLE 1. Wave and bed conditions of available experiments: Δ_k (mm) = roughness height and Λ_k (mm) = distance between the roughness elements.

The numerical procedure of predicting the friction velocity u_{fb} (hence α_b) is iterative:

(i) Calculate from the basic current f_c according to (2.15) for z_B^* given by fitting empirical data, and then compute the friction velocity $u_{fc} = \langle \bar{u}_0^* \rangle \sqrt{f_c/2}$, which gives the dimensionless friction velocity α_0.

(ii) Starting from $\alpha_c = \alpha_0$, we compute α_b from (10.11) by iteration. The value of Z_δ defined by (7.18) is found during the iteration.

(iii) Solve for $\bar{u}_c'$ according to (10.2).

(iv) Check if the discharge condition (6.4) is satisfied within the allowed error. If not, Step (ii) is repeated with a new trial α_c. The iteration procedure is continued until the discharge condition is satisfied. The solution of $\bar{u}_c'$ is then found.

(v) Compute the total mean velocity in the core from $\bar{u} = \epsilon \bar{u}_0 + \epsilon^2 \bar{u}_c'$.

In the next sections, we shall compare the predicted current profile at one station with available experiments, and predict further the velocity profiles at different stations in the direction of wave propagation.

11. Comparison with experiments

11.1. *Past experiments*

Laboratory studies in long flumes on wave-following currents have been reported by Bakker & Doorn (1978), Brevik & Aas (1980), Myrhaug, Reed & Fyfe (1987) and Mathisen & Madsen (1996*a*, *b*), only for the region near a rough bottom. Myrhaug *et al.* (1987) also reported results for the region near the smooth bottom. Measurements of the current velocity profile for the entire depth are more limited. We are aware of only two experiments by Kemp & Simons (1982, 1983) and by Klopman (1994, 1997) for rough beds. These experiments are classified in table 1, according to the empirical criteria of Kamphuis (1975). It is evident that only Kemp & Simons (1982) with smooth bed falls clearly in case A. Further discussions will be limited to the works of Kemp & Simons and Klopman.

Kemp & Simons have reported the current profiles for wave-following currents over smooth and rough beds (1982), and wave-opposing currents (1983) over a rough bed only, in a small wave tank of 14.5 m length, 0.457 m width and 0.69 m height. Roughness was created with 5 mm triangular strips separated at 18 mm intervals along the channel. The still water depth was 0.2 m. Along the centreline, the depth-averaged mean current velocity was $18.5\,\mathrm{cm\,s^{-1}}$ (1982) and $-11\,\mathrm{cm\,s^{-1}}$ (1983). The corresponding steady discharge rates were $Q = 0.037\,\mathrm{m^2\,s^{-1}}$ and $-0.022\,\mathrm{m^2\,s^{-1}}$

	Parameter	WCA1	WCA3	WCA4	WCA5
From data	ϵ	0.054	0.078	0.10	0.13
	α_0	1.009	0.49	0.29	0.21
	R	0.103	0.099	0.086	0.086
	Δ_{flux}	2.048	0.745	0.715	0.013
	$[\bar{u}]_+$	2.00	1.35	1.07	0.86
Calculated	$[\bar{u}]_+$	2.03	1.42	1.13	0.87
	Z_δ	8.54	8.65	8.81	9.00
	$k\delta \times 10^2$	2.37	2.26	2.11	1.9
	α_c	0.954	0.43	0.24	0.15

TABLE 2. Parameters of Kemp & Simons (1982) for wave-following current over a smooth bed. Wavelength $L = 1.23\,\mathrm{m}$, $k = 5.14\,\mathrm{m}^{-1}$, $C = 1.23\,\mathrm{m\,s}^{-1}$ and $kh = 1.03$. The four tests WCA1 to WCA5 are ordered by the wave steepness ϵ. WCA2 was not reported.

respectively. Waves with period $T = 1.006\,\mathrm{s}$ were added to the turbulent current. The wave amplitudes a ranged from 11.35 to 23.3 mm for the wave-following current of 1982, and 13.95 to 29.55 mm for the wave-opposing current of 1983. All full-depth profiles of currents were measured on top of a strip at a station 8.07 m away from the wavemaker. As shown in Ridler & Sleath (2000), for pure waves of similarly roughened bed, current profiles measured at different stations between two strips can be vastly different. Wave-affected current profiles may vary with the horizontal station. Such data is unfortunately unavailable for the full depth.

Klopman (1994) performed similar experiments in a larger wave flume 45 m long and 1 m wide. The still water depth was 0.5 m. The bed was roughened by coarse sand of 2 mm mean diameter. The test section was located at 22.5 m away from the wavemaker. The discharge was $Q = 0.08\,\mathrm{m^2\,s^{-1}}$. In the absence of waves, the mean velocity profile of the turbulent current was essentially logarithmic. A monochromatic wavetrain of period $T = 1.44\,\mathrm{s}$ and amplitude $a = 0.06\,\mathrm{m}$ was then superposed on the current which either followed or opposed the current. No tests with waves of other amplitude or frequency were reported. Later Klopman (1997) repeated the experiments under identical conditions, and also measured the transverse velocity with a view to examining Langmuir circulation due to the finite tank width. The mean velocity profile along the centreline was measured at the same station, but at only five different depths. The current velocities at all five measuring depths were, however, greater than the 1994 data by $0.0128\,\mathrm{m\,s}^{-1}$. We shall only use the more comprehensive measurements of Klopman (1994) for discussion. It is worth pointing out, however, that corresponding to the ratio a_b/k_N given in table 1, the ratio $\delta/k_N \sim 1.4$ is not large. Thus, the sand grains are not deeply immersed in the boundary layer.

Being the only full-depth observations available, the measurements by Kemp & Simons (1982, 1983) and Klopman (1994) are compared with our theory in the next section, despite the differences in seabed conditions.

11.2. *Wave-following current over a smooth bed by Kemp & Simons*

In table 2, the experimental parameters are summarized. Also included is the reflection coefficient R, which is $O(\epsilon)$ in all four cases. It is known (Mei 1989) that reflection of this intensity does not affect the induced streaming except at $O(\epsilon^2 R)$ which is negligible here. We also display the flux discrepancy Δ_{flux} which is a measure of the difference between the measured discharge and the theoretical current discharge, and

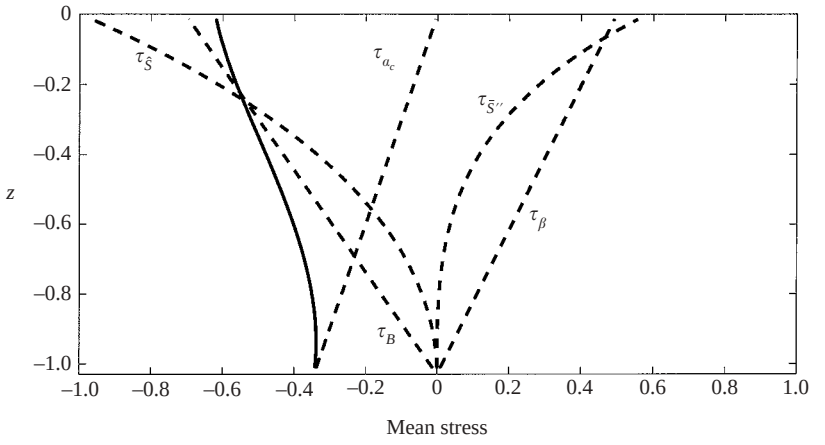

FIGURE 1. Various contributions to the mean stress for wave-opposing current over a smooth bed (Kemp & Simons 1982), run WCA5. —, total mean shear stress due to waves. The contributing factors are: $\tau_{\hat{S}}$, surface distortion of eddy viscosity; τ_{α_c}, change of friction velocity; τ_β, wave damping; τ_B, wave-induced Reynolds stress from BWBL; $\tau_{\bar{S}''}$, curvature of eddy viscosity due to vortex force.

is implied by (6.4) with $AA^* = 1$.

$$\Delta_{flux} = \frac{2\displaystyle\int_{-kh+k\delta}^{0} \bar{u}_c' \mathrm{d}z}{\coth(kh)} + 1. \tag{11.1}$$

When the measured value of $\bar{u_c}'$ is used in the preceding formula, departure from zero suggests difficulty in the velocity measurements. We also compare the values of $[\bar{u}]_+$ obtained from both theory and experiments to show that (7.15) can indeed provide good lower boundary value for the core current over a smooth bed.

To help understand the physics, let us first examine a typical stress distribution for the perturbed current, as defined in (10.1). Figure 1 shows the wave-induced mean stress for run WCA5. Both wave damping τ_β and curvature of the eddy viscosity $\tau_{\bar{S}''}$ are positive and increase from zero at the bed to their maximum at the water surface. Negative stresses, which tend to retard the current, are contributed by τ_{α_c}, τ_B and $\tau_{\hat{S}}$. Because of the surface distortion of eddy viscosity, $\tau_{\hat{S}}$ contributes the most to slow down the current near the water surface, while τ_{α_c} (also negative) in this case contributes little.

In figure 2, the velocity profiles of all reported runs by Kemp & Simons are compared with the predictions. The agreement between theory and experiments is quite good. In particular, the reduction of the current velocity near the free surface is predicted well. This suggests that not only the shear stress, but also the edge velocity, are described well, by (10.1) and (7.15), respectively. For run WCA1, the relative error in the total discharge Δ_{flux} is the largest, the agreement is poorer, probably owing to the smaller wave steepness and the smaller effects on the current.

No wave-opposing current profiles over a smooth bed have been reported by Kemp & Simons.

11.3. *Wave-following current over a rough bed by Kemp & Simons*

From Kemp & Simons (1982) a summary of experimental parameters is shown in table 3. The roughness height z_B is computed by fitting the measured velocity of pure

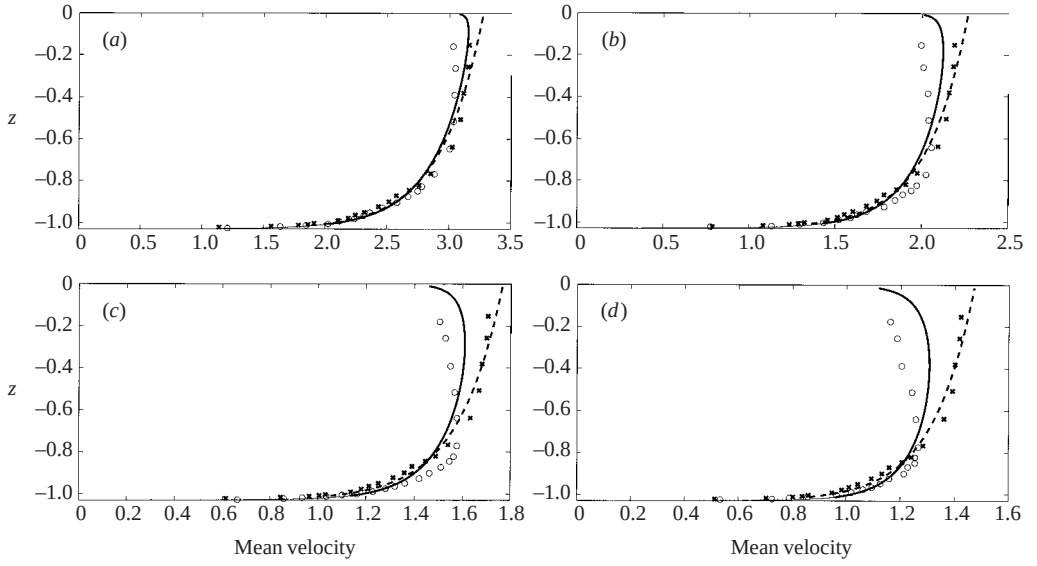

FIGURE 2. Comparisons with (*a*) WCA1, (*b*) WCA3, (*c*) WCA4 and (*d*) WCA5 of Kemp & Simons (1982) for wave-following current over a smooth bed. —, predicted current with waves; – – –, predicted pure current; ○, measured current with waves; ×, measured pure current.

	Parameter	WCR1	WCR3	WCR4	WCR5
From data	ϵ	0.06	0.08	0.10	0.13
	α_0	2.12	1.08	0.59	0.42
	R	0.088	0.078	0.074	0.072
	Δ_{flux}	8.102	4.268	1.312	0.205
	kz_r	0.13	0.15	0.13	0.15
	$\bar{u}_r$	2.13	1.7	1.21	0.92
	$[\bar{u}]_+$	1.70	1.33	1.03	0.77
Calculated	$[\bar{u}]_+$	0.47	0.14	0.13	0.19
	Z_δ	7.48	7.1	6.5	6.13
	$k\delta \times 10$	0.9	0.9	0.86	1.12
	α_c	1.50	0.46	0.29	0.29
	α_b	3.42	1.98	1.32	1.08

TABLE 3. Parameters of Kemp & Simons (1982) for wave-following current over a rough bed. Wavelength $L = 1.23\,\mathrm{m}$, $k = 5.14\,\mathrm{m}^{-1}$, $C = 1.23\,\mathrm{m\,s}^{-1}$, and $kh = 1.03$. Hydraulic roughness $z_B = 0.208\,\mathrm{cm}$ ($kz_B = 0.0105$). The four tests WCR1 to WCR5 are ordered by the wave steepness ϵ. WCR2 was not reported.

current with the logarithmic profile, with the tank bottom (the base of the strips) defined as $z = -kh$. Note that for the weaker waves: WCR1, WCR3 and WCR4, the flux discrepancy is very large, suggesting possible difficulty in measuring small velocity variations and boundary-layer effects near the sidewalls. Comparisons are only shown for runs WCR4 and WCR5. It also turns out that the lower boundary value $[\bar{u}'_c]_+$ given by (7.15) differs markedly from the data, see table 3. By using the measured velocity $\bar{u}_r$ at a reference height z_r, shown in the same table, a fair agreement between predicted and measured velocities is achieved, as shown in figure 3. The need for this empirical fitting is not surprising since the profiles were all measured at the station

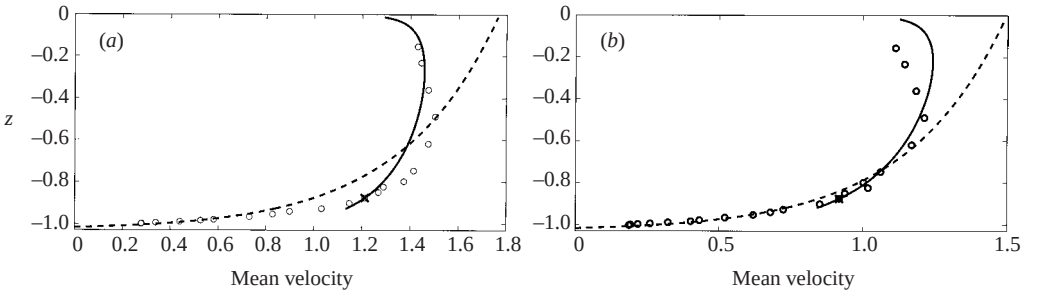

FIGURE 3. Profiles of wave-following current over a rough bed by Kemp & Simons (1982), runs (*a*) WCR4 and (*b*) WCR5. —, theoretical profile with waves; - - -, theoretical profile of pure current; ○, measured profile with waves; ×, height (kz_r) where empirical fitting with ($\bar{u}_r$) is made.

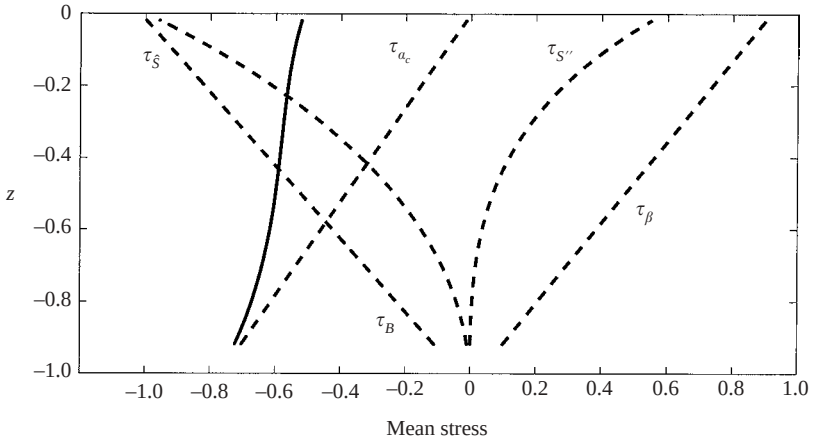

FIGURE 4. Predicted contributions to the mean stress for run WCR5 of Kemp & Simons (1982). —, total mean shear stress due to waves. Various contributing parts are: $\tau_{\hat{S}}$, surface distortion of eddy viscosity; τ_{α_c}, change of friction velocity; τ_β, wave damping; τ_B, wave-induced Reynolds stress from the bottom wave boundary-layer; $\tau_{\bar{S}''}$, curvature of the eddy viscosity due to vortex force.

where a strip is located, and are most probably different from the profiles at other stations between the strips. With similar fitting, the agreement is, of course, worse, for run WCR4 than for run WCR5 in view of the very large discharge error Δ_{flux} for the former.

To help understand the physics, we plot in figure 4 various wave-induced stress components as defined in (10.1), for case WCR5. Note that τ_β and $\tau_{\bar{S}''}$ are again both positive and the greatest near the free surface. All these tend to increase the current speed near the free surface. τ_B is negative, but is almost cancelled by τ_β. Owing to waves, the dimensionless core friction velocity α_0 is smaller than α_0 of the pure current ($\alpha_c - \alpha_0 = 0.29 - 0.42 = -0.13$). Thus, τ_{α_c} attains the negative maximum at the bottom. Most importantly, the shear stress $\tau_{\hat{S}}$ due to the distortion of eddy viscosity is negative and large and is the dominating factor for reducing the current velocity near the free surface. The combined effect is much stronger than the case over a smooth bed.

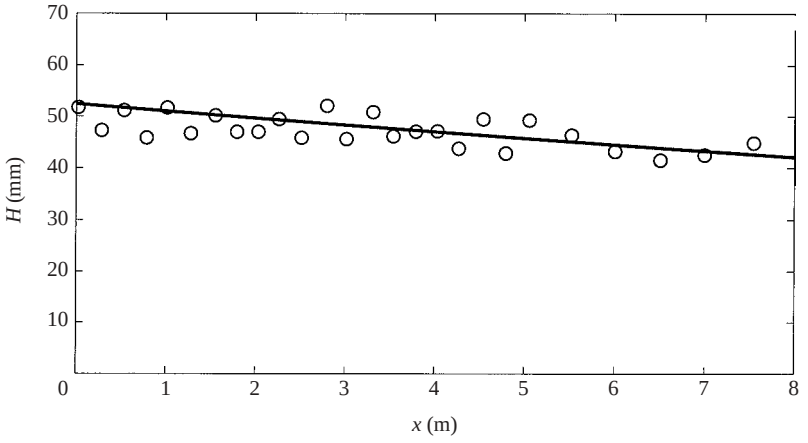

FIGURE 5. Wave height attenuation for case WCR5: ○, Measured wave height; —, predicted wave height.

	Parameter	WDR1	WDR2	WDR3	WDR4	WDR5
From data	ϵ	0.07	0.09	0.10	0.13	0.15
	α_0	0.84	0.55	0.43	0.26	0.19
	R	0.025	0.03	0.023	0.026	0.02
	Δ_{flux}	1.610	0.520	−0.309	−0.222	0.104
	kz_r	0.13	0.18	0.15	0.18	0.15
	$\bar{u}_r$	−0.59	−0.67	−0.55	−0.45	−0.32
	$[\bar{u}_c]_+$	−0.500	−0.471	−0.469	−0.357	−0.285
Calculated	$[\bar{u}_c]_+$	−0.550	−0.390	−0.284	−0.269	−0.242
	Z_δ	6.8	6.62	6.45	6.00	5.62
	$k\delta \times 10$	0.92	1.08	1.07	1.20	1.22
	α_c	1.32	0.86	0.64	0.47	0.36
	α_b	2.75	2.02	1.67	1.22	0.97

TABLE 4. Parameters of Kemp & Simons (1983) for wave-opposing current over rough bottom. Wavelength $L = 1.23\,\mathrm{m}$, $k = 5.14\,\mathrm{m}^{-1}$, $C = 1.23\,\mathrm{m\,s}^{-1}$, and $kh = 1.03$. Hydraulic roughness $z_B = 0.203\,\mathrm{cm}$ ($kz_B = 0.0104$). The five tests WDR1 to WDR5 are ordered by the wave steepness ϵ.

Although the current profiles were measured only at a single station, records are available for the wave height along the channel, for run WCR5 only. In terms of the normalized slow coordinate x_2, the length of the tank is only $\Delta x_2 = 0.69$. Hence, we use the damping coefficient β computed for the starting station $x_2 = 0$ for calculating the wave attenuation. The predicted and measured wave heights are shown in figure 5. The reasonable agreement gives partial confirmation of the boundary-layer model which predicts comparable importance of dissipation in the bottom boundary layer and in the core.

11.4. *Wave-opposing current over a rough bed by Kemp & Simons*

A summary of dimensionless parameters for all the wave-opposing current tests, both given and predicted, is given in table 4.

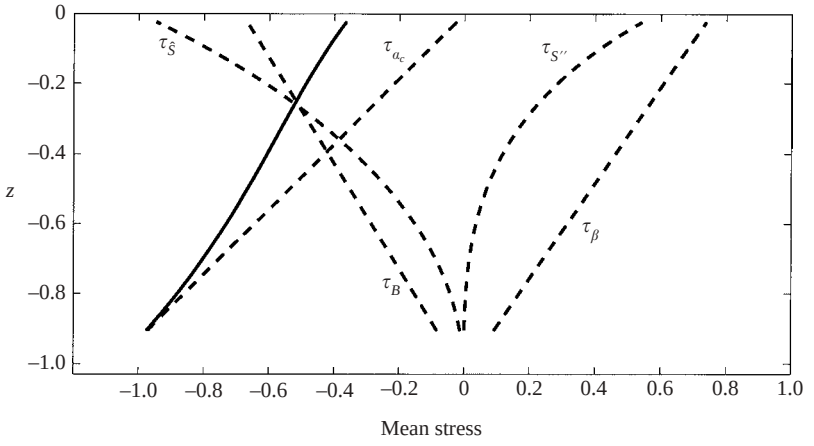

FIGURE 6. Various contributions to the mean stress for wave-opposing current over rough bottom of Kemp & Simons (1983), case WDR5. —, the total mean shear stress due to waves. The contributing factors are: $\tau_{\hat{S}}$, surface distortion on the eddy viscosity; τ_{α_c}, change of the friction velocity in the core region; τ_β, wave damping; τ_B, wave-induced Reynolds stress from the BWBL; $\tau_{\bar{S}''}$, curvature of the eddy viscosity.

Note that the discharge discrepancy is relatively small in all cases. Using input parameters computed from data as listed in table 2, numerical results are obtained for the various components of the shear stresses and the current velocity profile. The predicted parameters α_c and α_b are also recorded in table 4. Also, in these runs, the predicted $[\bar{u}]_+$ nearly equals the measured value at the same station with a strip. This coincidence can only be accidental in view of the separation of strips.

Let us first examine, for the representative run WDR5, the stress distribution for the perturbed current, as defined in (10.1). Again both wave damping τ_β and curvature of the eddy viscosity $\tau_{\bar{S}''}$ are positive, but they now tend to slow down the current. They both attain their maximum at the water surface and vanish at the bottom.

Negative stresses, which tend to speed up the current, are contributed by τ_{α_c}, τ_B and $\tau_{\hat{S}}$. Again, τ_B due to the wave-induced Reynolds stress at the outer edge of the BWBL, nearly cancels the opposite effect of τ_β (figure 6). The negative stress due to the surface distortion of eddy viscosity $\tau_{\hat{S}}$ contributes the most to speed up the current near the water surface. Now since $\alpha_c - \alpha_0 = 0.36 - 0.19 = 0.17$, τ_{α_c} attains a very large negative maximum at the bottom, contributing to the flattening of the velocity profile near the bed, in comparison with the pure current. The net shear stress shown by a solid line is negative throughout the entire depth, but more so than the wave-following case of WCR5. Now the negative shear stress near the free surface also causes the surface current to be stronger than that of a pure current. Figure 7 compares the predicted current profile $\bar{u}_0 + \epsilon\bar{u}_c'$, with the measured data by Kemp & Simons for case (WDR5). The velocity profile of a pure current (logarithmic, dotted) is also included for reference. The overall agreement between the theory and experiments is very good. Reduction near the bottom and increase near the surface of the mean velocity are correctly predicted. Note in table 2, that there is an increase in friction velocity due to waves, i.e. $\alpha_b > \alpha_c$, which is responsible for the reduction of the mean current velocity near the bed, consistent with most past observations, contributing to an increase of the apparent bottom roughness (Grant & Madsen 1986).

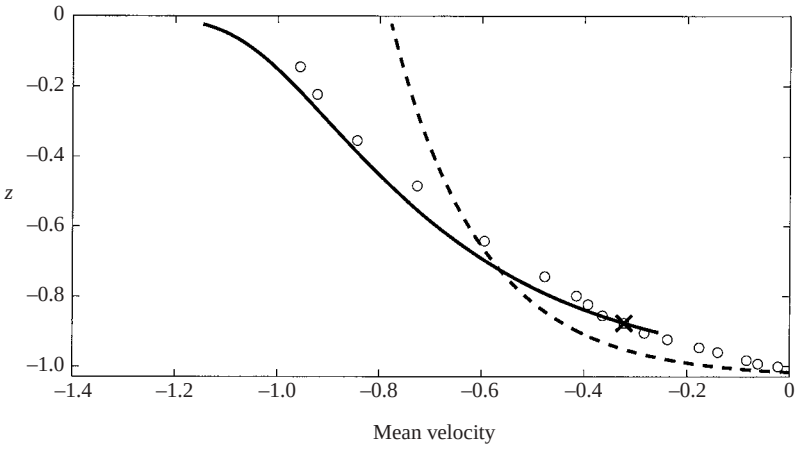

FIGURE 7. Current profile of WDR5 by Kemp & Simons (1983) for wave-opposing current over a rough bed. —, theoretical profile; - - -, theoretical profile of pure current; ○, measured profile; ×, height (kz_r) where empirical fitting with ($\bar{u}_r$) is made.

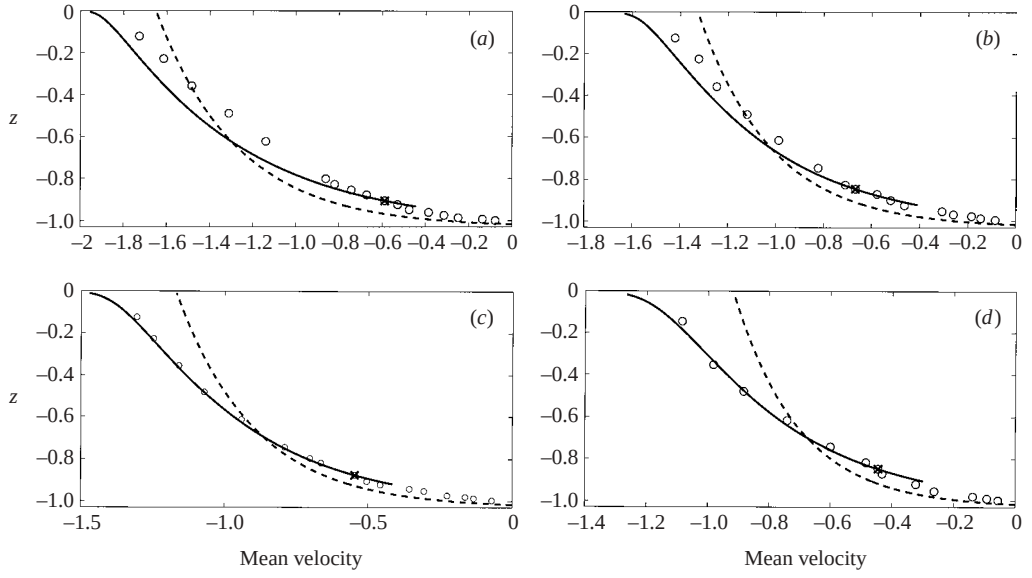

FIGURE 8. Current profiles for wave-opposing current over a rough bed. —, predicted profile with waves; - - -, predicted profile of pure current; ○, measured profile with waves; ×, height (kz_r) where empirical fitting with ($\bar{u}_r$) is made. (*a*) WDR1; (*b*) WDR2; (*c*) WDR3; (*d*) WDR4.

Additional comparisons for all other runs WDR1–WDR4 are presented in figure 8, with satisfactory agreement. The stress distributions resemble those shown in figure 6 and are omitted.

For run WDR4, the attenuation of wave height $H = 2a$ with distance has been reported by Kemp & Simons (1983) . In terms of the normalized slow variable x_2, the length of the tank is $\Delta x_2 = 0.93$. Using the damping coefficient β at $x_2 = 0$ (the current-measuring station at mid tank), we compare in figure 9 the computed H and those measured against the distance from the wavemaker. The agreement

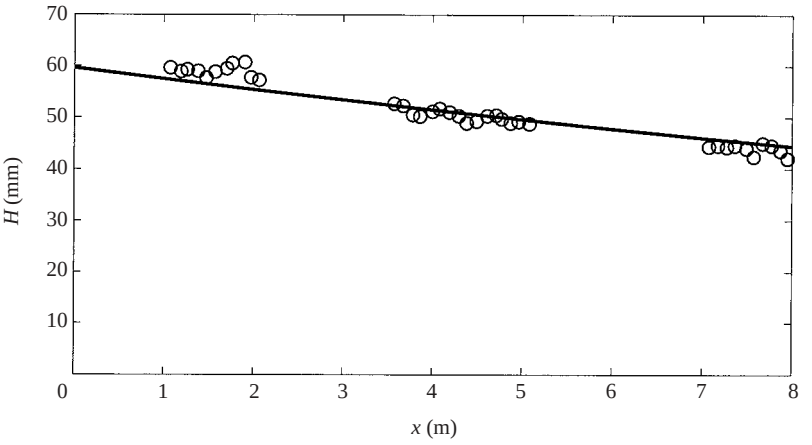

FIGURE 9. Wave height attenuation of WDR4. —, theoretical wave height; ○, measured wave height.

	Parameter	Wave-following current	Wave-opposing current
From data	ϵ	0.14	0.14
	α_0	0.119	0.119
	R	<0.02	<0.02
	Δ_{flux}	0.021	0.066
	kz_r	0.14	0.10
	$\bar{u}_r$	0.56	−0.40
	$[\bar{u}_c]_+$	0.4	−0.2
Calculated	$[\bar{u}_c]_+$	0.06	−0.24
	Z_δ	4.06	4.24
	$k\delta \times 10^2$	3.74	3.86
	α_c	0.06	0.24
	α_b	0.47	0.56

TABLE 5. Parameters of Klopman (1994) for wave-following and wave-opposing currents over a rough bed. Dimensionless hydraulic roughness $kz_B = 9.2 \times 10^{-4}$.

between prediction and data is good, confirming again the comparable importance of dissipation within the boundary layer and in the core above.

For WDR4, the eddy viscosity near the bottom was reported by Kemp & Simons (1983). The scatter of data was so large that no meaningful comparison with theory can be made.

11.5. *Wave-following/opposing currents over a rough bed by Klopman*

In Klopman (1994), the wavenumber is $k = 2.34\,\mathrm{m}^{-1}$ according to the linear wave theory. The bottom is roughened by sand of diameter 2 mm. Other experimental and calculated parameters are summarized in table 5. From table 5, we find $\delta/k_N \sim 1.4$ for both wave-following and opposing currents. Therefore, wave-induced turbulence is probably three dimensional. Nevertheless after fitting the velocity at one height, z_r, the predicted mean velocity profile compares with Klopman's data very well for both wave-following and wave-opposing currents, as shown in figure 10.

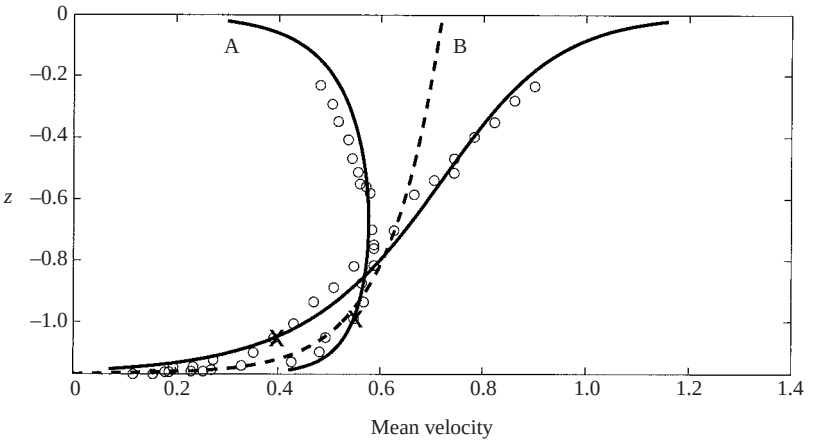

FIGURE 10. Comparisons with Klopman (1994) for wave-following and wave-opposing currents. In this figure the basic current is from left to right. A, waves are from left to right; B, waves are from right to left; —, theoretical profile with waves; - - -, theoretical profile of pure current; ○, experimental data for currents with waves; ×, heights (kz_r) where empirical fitting with ($\bar{u}_r$) are made.

12. Longitudinal variation of current

In all the existing experiments cited here, current measurements for the full depth were made only at a single station. In view of the empirical assumptions required in the theory, it would be desirable to have new measurements at many stations in order to provide firmer checks. For this purpose, we have extended our calculations to include the change of the current profiles along the channel, provided that the wave and current conditions are specified at one station. Predictions are shown only for a smooth bed.

Recalling the definition of $x_2 = k^3a^2x^*$, we start from station $x_2 = 0$ where $A(0) = 1$ and advance to larger $x_2 > 0$ in the direction of wave propagation. For a smooth bed, the discharge of the pure current, or the depth-averaged velocity $\bar{u}_0^*$, can be specified so that α_0 can be easily computed. Afterwards, the numerical algorithm to compute $\bar{u}(x_2)$ is straightforward. Let the wave and current conditions be known at $x_2 = X_{k-1}$. To predict the current velocity at $x_2 = X_k = X_{k-1} + \Delta x_2$, we first compute the wave amplitude $A(X_k) = A(X_{k-1}) - \beta(X_{k-1})\Delta x_2/2$, where $\beta(X_{k-1})$ is the energy dissipation rate at $x_2 = X_{k-1}$. Then $\alpha_c(X_k)$ and $\alpha_b(X_k)$ are calculated by the procedures described in § 10.3.

Two examples are presented in figure 11 for a smooth bed. One is for the wave-following current and the other for the wave-opposing current. The wave and current conditions at the start ($x_2 = 0$) are the same as those in run WCA5 of Kemp & Simons (1982). In both cases, as the distance from $x_2 = 0$ increases, the current profile approaches the limit of a pure current without waves. Reduction or increase of the current velocity near the bottom becomes smaller and smaller. When the waves are eventually damped out, the current profile becomes logarithmic in depth. Note that the total Eulerian flux decreases (increases) with distance when waves and current have the opposite (same) direction, as expected by mass conservation (6.4).

Similar predictions have been made for a rough bed and with very large a_b/k_N, for possible comparisons with future experiments in a large flume or in the field. Results resemble those in figure 11 and are not presented.

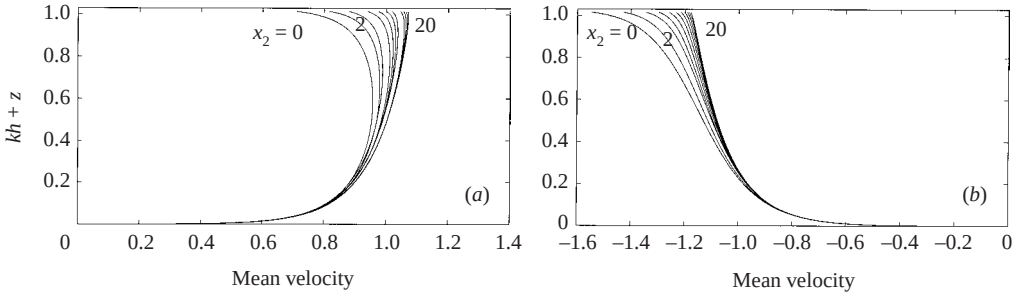

FIGURE 11. Changes along the tank. The damping scale x_2 is defined by $x = \epsilon^2 x_2$ and the spatial grid step is $\Delta x_2 = 2$.

13. Concluding remarks

In this paper, an analytical boundary-layer theory for predicting the wave effects on a turbulent current over a smooth or rough bed has been presented. The current is assumed to be as strong as the orbital velocity of waves and renders the flow turbulent throughout the depth. For a smooth bed, a model of continuous eddy viscosity parabolic in depth is used. For a rough bed, a discontinuous eddy viscosity is used instead to account for the combined effects of waves and current in the bed wave-boundary layer. At the leading order, turbulence in both the bed boundary layer and the core results in wave attenuation over a long distance of many wavelengths. At the second order, waves modify the mean flow through wave-induced Reynolds stresses due to oscillations in all regions of the flow. In particular, the perturbed mean turbulent stress is not zero on the still water surface despite the absence of wind, and is not constant in depth above the bottom boundary layer. It is of special importance that this mean shear stress on the free surface is opposite in direction to the waves. As a consequence, a wave-following current must experience a reduction, while a wave-opposing current experiences an increase, in speed. This phenomenon is due largely to the distortion of eddy viscosity at the free surface.

Comparison with existing experiments for a smooth bed is successful. For a rough bed, the roughness elements in existing experiments are either relatively large or well separated, making a boundary-layer analysis difficult. Nevertheless, the present theory still gives a good prediction of current for the entire depth, if empirical matching is made at one depth just above the bed boundary layer (as in Grant & Madsen). For beds roughened by well separated strips, this theory appears adequate for predicting quantities that vary slowly in the horizontal direction, such as the attenuation rate, and may give a good prediction of the horizontally averaged velocities profiles, without empirical fitting. To check this speculation, additional measurements either for deeply submerged roughness, or of current profiles at several closely spaced stations between strips and over a long fetch, would be worthwhile.

Extension of this study to the three-dimensional problem of Langmuir circulation in shallow water is of value to the transport of fine sediments in lakes and coastal waters, and is underway.

We are grateful for the financial support by US Office of Naval Research (Grant N00014-89J-3128, directed by Dr Thomas Swean) and US National Science Foundation (Grant CTS-0075713, directed by Professors John Foss, C. F. Chen and M. Plesniak). We also acknowledge the kind assistance from Professor J. A. Battjes of Delft University of Technology and Professor R. Simons of University College

of London for supplying us with the original experimental data cited herein. Our indebtedness to Professor O. S. Madsen of MIT for many fruitful discussions is also recorded here with pleasure.

Appendix A. Mechanical energy in waves

We sketch here the derivation of the mechanical energy equation (5.5). For brevity, let us use the index notation for the dimensionless coordinates and the total fluid velocties $x_1 \equiv x, x_3 \equiv z; q_1 \equiv u, q_3 \equiv w$ and rewrite the exact continuity and momentum equations (3.2), (3.3) and (3.4). Following the standard procedure (see e.g. Mei 1989), it can be shown that the depth-integrated total energy budget reads

$$\frac{\partial}{\partial t}\int_{z_+}^{\eta}\left(\frac{q_i^2}{2}+\frac{gk}{\omega^2}\frac{\eta^2}{2}\right)\mathrm{d}z = -\frac{\epsilon^2}{2}\int_{z_+}^{\eta}\alpha S\left(\frac{\partial q_i}{\partial x_j}+\frac{\partial q_j}{\partial x_i}\right)^2\mathrm{d}z + \frac{\partial}{\partial x}\int_{z_+}^{\eta}\left(q_i\sigma_{i1}-q_1\frac{q_i^2}{2}\right)\mathrm{d}z, \tag{A 1}$$

where $z_+ = z_b - kh$ denotes the bed and $\sigma_{ij} = -p\delta_{ij} + \tau_{ij}$ the total stress tensor. Invoking periodicity, and using continuity, the period-averaged energy budget is, exactly,

$$\frac{\epsilon^2}{2}\overline{\int_{z_+}^{\eta}\alpha S\left(\frac{\partial q_i}{\partial x_j}+\frac{\partial q_j}{\partial x_i}\right)^2\mathrm{d}z} = \overline{\frac{\partial}{\partial x}\int_{z_+}^{\eta}\left(-\delta_{i1}pq_i+\epsilon^2\alpha S\left(\frac{\partial q_1 q_i}{\partial x_i}+\frac{\partial q_i^2/2}{\partial x_1}\right)-q_1\frac{q_i^2}{2}\right)\mathrm{d}z}. \tag{A 2}$$

Thus, on average, dissipation by turbulence in a fluid column of small width is balanced by the net total stress working and energy flux on both sides.

We first substitute in (A 2) $q_i = \bar{q}_i, \eta = \bar{\eta}$ and $p = \bar{p}$ to obtain the energy budget for the steady current, noting that $\bar{q}_1 = \bar{u}(z), \bar{q}_3 = \bar{w} = 0$ and $\partial\bar{p}/\partial x \neq 0$. We then substitute in (A 2) $q_i = \bar{q}_i + \tilde{q}_i$, $\eta = \bar{\eta} + \tilde{\eta}$ and $p = \bar{p} + \tilde{p}$ for the energy budget of the total flow. The difference of the two results is the energy budget of the waves. Making use of the following identity

$$\int_{z_+}^{\bar{\eta}+\tilde{\eta}} f\,\mathrm{d}z = \int_{z_+}^{0} f\,\mathrm{d}z + \int_{0}^{\bar{\eta}+\tilde{\eta}} f\,\mathrm{d}z \tag{A 3}$$

and the order estimates,

$$\tilde{q}_i, \bar{q}_i, \tilde{\eta} = O(\epsilon), \quad \bar{\eta} = O(\epsilon^2), \quad \tilde{S} = O(\epsilon), \quad \frac{\partial \bar{f}}{\partial x} = O(\epsilon^2), \tag{A 4}$$

we obtain the time-averaged wave energy budget

$$\frac{\epsilon^2}{2}\int_{z_+}^{0}\alpha\bar{S}\overline{\left(\frac{\partial\tilde{q}_i}{\partial x_j}+\frac{\partial\tilde{q}_j}{\partial x_i}\right)^2}\mathrm{d}z = -\frac{\partial}{\partial x}\int_{z_+}^{0}\overline{\tilde{u}\tilde{p}}\,\mathrm{d}z + O(\epsilon^5) \tag{A 5}$$

which is (5.5).

Appendix B. Unimportance of surface wave boundary layer

We first list the exact dimensionless boundary conditions, normalized by core scales (cf. (2.4), (2.5) and (2.6)). Dynamically, the tangential and normal stresses must vanish

on the moving wind-free surface,

$$-[-P+\tau_{xx}]\frac{\partial\eta}{\partial x}+\tau_{xz}=0, \quad z=\eta, \tag{B 1}$$

$$[-P+\tau_{zz}]-\tau_{xz}\frac{\partial\eta}{\partial x}=0, \quad z=\eta, \tag{B 2}$$

where P is the total pressure (static and dynamic). In addition, the kinematic surface boundary condition requires

$$\frac{\partial\eta}{\partial t}+u\frac{\partial\eta}{\partial x}-w=0, \quad z=\eta. \tag{B 3}$$

Let us denote the boundary-layer corrections of the flow field by (U', W', P'), i.e.

$$u=u_c+U', \quad w=w_c+W', \quad p=p_c+P', \tag{B 4}$$

where (u_c, w_c, p_c) are the values of (u, w, p) evaluated at the outer edge of the surface boundary layer, where all correction terms should vanish.

First, the oscillatory shear stress must vanish on the free surface, hence,

$$\frac{\partial\tilde{u}_c}{\partial z}=O\left(\frac{\partial\tilde{U}'}{\partial z}\right). \tag{B 5}$$

In view of the smallness of the eddy viscosity, $O(\epsilon^2 k\delta)$, where the dimensionless boundary-layer thickness near the free surface is also of the order $k\delta=O(\epsilon^2)$, we have, within the surface wave boundary layer

$$\tilde{U}'=O(\epsilon^2\tilde{u}_c)=O(\epsilon^3). \tag{B 6}$$

Now the mean current. The boundary-layer correction to the perturbed core current is the result of nonlinear interaction between the irrotational waves and the boundary-layer corrections, hence

$$\bar{U}'=O(\epsilon\tilde{U}')=O(\epsilon^4). \tag{B 7}$$

The continuity equations for the surface layer corrections to the oscillatory and the mean motions are, respectively,

$$\frac{\partial\tilde{U}'}{\partial x}+\frac{\partial\tilde{W}'}{\partial z}=0, \quad \frac{\partial\bar{U}'}{\partial x}+\frac{\partial\bar{W}'}{\partial z}=0. \tag{B 8}$$

From these we find

$$\tilde{W}'=O(\epsilon^2\tilde{U}')=O(\epsilon^5), \quad \bar{W}'\leqslant O(\epsilon^2\bar{U}')\leqslant O(\epsilon^6). \tag{B 9}$$

From the vertical momentum equation for the surface-layer corrections, the following order of magnitude estimate is obtained

$$\tilde{W}'\sim\frac{\partial\tilde{P}'}{\partial z}. \tag{B 10}$$

Since $\Delta z=O(\epsilon^2)$, it follows that

$$\tilde{P}'=O(\epsilon^2\tilde{W}')=O(\epsilon^7). \tag{B 11}$$

We further estimate that $\bar{P}'=O(\epsilon\tilde{P}')=O(\epsilon^8)$ because the perturbed mean boundary layer correction is due to the nonlinear interaction between the irrotational waves and the perturbed wave boundary-layer corrections.

In view of the smallness of the correction terms, only the outer solution suffices near the free surface up to the desired accuracy.

REFERENCES

Abramowitz, M. & Stegun, I. (ed.) 1972 *Handbook of Mathematical Functions*. Dover.

Bakker, W. T. & Doorn, T. V. 1978 Near-bottom velocities in waves with a current. In *16th Conf. on Coastal Engng*, pp. 1394–1413.

Brevik, I. & Aas, B. 1980 Flume experiment on waves and currents, 1, rippled bed. *Coastal Engng* **3**, 149–177.

Dingemans, M. W., Kester, J. A. T. M. V., Radder, A. C. & Uittenbogaard, R. E. 1996 The effect of the CL-vortex force in 3d wave–current interaction. In *Coastal Engineering: Proc. 25th Intl Conf.*, pp. 4821–4832. ASCE.

van Duin, C. A. & Janssen, P. A. E. M. 1992 An analytical model of the generation of surface waves by turbulent air flow. *J. Fluid Mech.* **236**, pp. 197–215.

Grant, W. D. & Madsen, O. S. 1979 Combined waves and current interaction with a rough bottom. *J. Geophys. Res.* **84** (C4), 1797–1808.

Grant, W. D. & Madsen, O. S. 1986 The continental-shelf bottom boundary layer. *Annu. Rev. Fluid Mech.* **18**, 265–305.

Groeneweg, J. & Battjes, J. A. 2003 Three-dimensional wave effects on a steady curent. *J. Fluid Mech.* **478**, 325–343.

Groeneweg, J. & Klopman, G. 1998 Changes of the mean velocity profiles in the combined wave–current motion in a GLM formulation. *J. Fluid Mech.* **370**, 271–296.

Jacobs, S. J. 1987 An asymptotic theory for the turbulent flow over a progressive water waves. *J. Fluid Mech.* **1974**, 69–80.

Jonsson, I. 1966 Wave boundary layers and friction factors. In *Proc. 7th Conf. on Coastal Engineering*, pp. 127–148.

Kajiura, K. 1968 A model of the bottom boundary layer in water waves. *Bull. Earthquake Res. Inst.* **46**, pp. 75–123.

Kamphuis, J. 1975 Friction factors under oscillatory waves. *Proc. ASCE J. Waterway, Harbors Coastal Engng Div.* **101**, 135–144.

Kemp, P. H. & Simons, R. R. 1982 The interaction between waves and a turbulent current: waves propagating with the current. *J. Fluid Mech.* **116**, 227–250.

Kemp, P. H. & Simons, R. R. 1983 The interaction between waves and a turbulent current: waves propagating against the current. *J. Fluid Mech.* **130**, 73–89.

Klopman, G. 1994 Vertical structure of the flow due to waves and currents: Laser-doppler flow measurements for waves following or opposing a current. *Tech. Rep.* H840.32, Part 2. Delft Hydraulics.

Klopman, G. 1997 Secondary circulation of the flow due to waves and current: laser-Doppler flow measurements for waves following or opposing a current. *Tech. Rep.* Z2249. Delft Hydraulics.

Liu, A.-K. & Davis, S. H. 1977 Viscous attenuation of mean drift in water waves. *J. Fluid Mech.* **81**, 63–84.

Mathisen, P. P. & Madsen, O. S. 1996*a* Waves and currents over a fixed rippled bed: bottom roughness experienced by waves in the presence and absence of currents. *J. Geophys. Res.* **101** (C7), 16 533–16 542.

Mathisen, P. P. & Madsen, O. S. 1996*b* Waves and currents over a fixed rippled bed: bottom roughness experienced by currents in the presence waves. *J. Geophys. Res.* **101** (C7), 16 543–16 550.

Mei, C. C. 1989 *The Applied Dynamics of Ocean Surface Waves*, 2nd edn. World Scientific.

Miles, J. 1993 Surface-wave generation revisited. *J. Fluid Mech.* **256**, 427–441.

Myrhaug, D., Reed, K. & Fyfe, A. J. 1987 Seabed boundary layer studies for pipelines: large scale laboratory experiments. In *Proc. Intl Symp. on Offshore Engng*, pp. 345–359. Rio de Janeiro, Brasil.

Nepf, H. M., Cowen, E. A., Kimmel, S. J. & Monismith, S. G. 1995 Longitudinal vortices beneath breaking waves. *J. Geophys. Res.* **100** (C8), 16 211–16 221.

Nielsen, P. & You, Z. J. 1996 Eulerian mean velocity under non-breaking waves on horizontal bottom. In *Coastal Engineering: Proc. 25th Intl Conf.*, pp. 4066–4078. ASCE.

Phillips, O. M. 1977 *The Dynamics of the Upper Ocean*, 2nd edn. Cambridge University Press.

Ridler, E. L. & Sleath, J. F. A. 2000 Effect of bed roughness on time-mean drift induced by waves. *J. Waterway, Port, Coastal and Ocean Engng* **126**, 23–29.

Sleath, J. 1984 *Sea Bed Mechanics*. John Wiley.

Tang, Y. & Grimshaw, R. 1999 Recent developments in the theory and modelling of storm surges. In *Modelling Coastal Sea Processes* (ed. J. Noye), pp. 135–158. World Scientific.

Townsend, A. A. 1972 Flow in a deep turbulent boundary layer over a surface distorted by water waves. *J. Fluid Mech.* **55**, 719–735.